

Testing for Extreme Volatility Transmission with Realized Volatility Measures

Christophe Boucher*, Gilles de Truchis †, Elena Dumitrescu ‡, Sessi Tokpavi §

January, 2018

Abstract

This paper proposes a simple and parsimonious semi-parametric testing procedure for variance transmission. Our test focuses on conditional extreme values of the unobserved process of integrated variance since they are of utmost concern for policy makers due to their sudden and destabilizing effects. The test statistic is based on realized measures of variance and has a convenient asymptotic χ^2 distribution under the null hypothesis of no Granger causality, which is free of estimation risk. Extensive Monte Carlo simulations show that the test has good small sample size and power properties. An extension to the case of spillovers in quadratic variation is also developed. An empirical application on extreme variance transmission from US to EU equity markets is further proposed. We find that the test performs very well in identifying periods of significant causality in extreme variance, that are subsequently found to be correlated with changes in US monetary policy.

JEL Codes: C12, C32, C58

Keywords: Extreme volatility transmission, Granger causality, Integrated variance, Realized variance, Semi-parametric test, Financial contagion.

*christophe.boucher@parisnanterre.fr, EconomiX, UPL, Univ. Paris Nanterre, CNRS, F92000 Nanterre, France.

†detruchis.gilles@parisnanterre.fr, EconomiX, UPL, Univ. Paris Nanterre, CNRS, F92000 Nanterre, France.

‡elena.dumitrescu@parisnanterre.fr, EconomiX, UPL, Univ. Paris Nanterre, CNRS, F92000 Nanterre, France.

§Corresponding author: sessi.tokpavi@univ-orleans.fr, LEO, University of Orléans, CNRS, 45100 Orlans, France.

1 Introduction

The detection of *volatility* (and more generally *risk*) *transmission* across assets and markets and the understanding of the spillover mechanisms is key in finance and macroeconomics. A main reason for this is that volatility spillovers are thought to have potential adverse effects on financial stability, especially in the current context of increasing financial integration.

A pioneer work in this field is Granger et al. (1986) who introduce the concept of Granger-causality in variance, that is defined in terms of incremental predictive ability. This paved the way for a growing literature focused on developing statistical procedures to test for variance transmission (e.g. Engle and Ng, 1988; Engle et al., 1990; Cheung and Ng, 1996; Hong, 2001; Sensier and van Dijk, 2004; Hafner and Herwartz, 2008). Although highly predictable, return variance is inherently unobservable and traditionally estimated by fitting parametric econometric models such as GARCH. All these causality tests are easy to implement, but sensitive to misspecifications in the conditional mean and variance equations and assume that realizations in the upper and lower tails of the distribution are generated by the same process.

As an alternative to the GARCH family of models, in recent years it has become common practice to use high-frequency data when making inference about the variation of financial asset prices. This opened the way for new causality in variance testing procedures that exploit the success of (nonparametric) realized volatility measures in estimating the true latent process of volatility. Corradi et al. (2012) develop a nonparametric density test for conditional independence between two daily realized measures of volatility. Their approach allows to control for the effect of jumps and microstructure noise in the log-price process when testing for spillover effects in the integrated variance, hereafter IV , the continuous part of the quadratic variation, hereafter QV .

However, Corradi et al. (2012) test for volatility transmission by looking at the whole volatility distribution, without disentangling the tail dependence behaviour from that of the center of the distribution. A different conditional density for IV when conditioning also on another asset's past IV instead of exclusively on the first asset's past IV can be due to spillovers in the center of the distributions or in the tails, the latter being of outmost concern for financial markets participants. It is well known that financial market co-movements increase during turbulent periods and they can be seen as a device that amplifies risk instead of dispersing it during crisis periods (see Cappiello et al., 2014; Forbes and Rigobon, 2002; Baele, 2005). In the context of Granger causality testing, this comes down to saying that causality between the tails of the distributions is generally quite different from causality between the centers of the distributions and in empirical practice users could largely benefit

from causality tests that allow to distinguish between the two. In other words, compared to the approach of Corradi et al. (2012), an inferential procedure that is designed to check for causality in the center (the tails) of the volatility distribution should be more powerful when causality indeed operates in the center (the tails).

Our paper hence contributes to the existing literature by proposing a semi-parametric testing procedure to check for causality in the upper tail of the volatility distribution (conditional extreme variance) by making use of realized variance measures.¹ The inference is based on a Ljung and Box (1978)-type test statistics that checks for cross-lagged correlation between realized variance exceedances. These can be defined as upper-tail event variables that take the value one when the associated asset prices register periods of extreme volatility, i.e. when the realized variance measure goes beyond its conditional quantile, and zero otherwise. In particular, the test directly exploits the asymptotic theory for high-frequency realized measures and the fact that the realized variance is a highly persistent process whose conditional quantiles are simple to estimate in a Heterogeneous Quantile Autoregressive framework (see Zikes and Barunik, 2014). Under standard regularity assumptions including the IIDness of the microstructure noise, we show that the proposed test statistic has an asymptotic chi-square distribution. The additional estimation steps do not influence the asymptotic behavior of our test statistics, i.e., the asymptotic distribution of the test based on realized measures and their estimated quantiles is the same as the one based on the unobservable price variability measures and their quantiles. In particular, the estimation risk vanishes asymptotically, if the intra-daily time dimension, M , used for the computation of the realized measures of variance, and the daily sample-size T , go to infinity.

Our procedure has several appealing features. It doesn't impose any assumptions on the distributions of the financial returns since it is based only on non-parametric and semi-parametric estimation methods. It insures a good power against alternatives of extreme variance spillover by checking for causality in a reasonably large number of lags. Our procedure is also very easy to implement, as realized measures of variation have gained wide popularity in the financial econometrics literature and they can be easily computed with free toolboxes such as the Oxford MFE Matlab Toolbox by Kevin Sheppard, while the Heterogeneous Quantile Autoregressive model comes down to implementing a traditional quantile regression model with averaged lagged endogenous variables. As a byproduct, the user can rely on our testing procedure to identify causality in the discontinuous (jumps) component of the unobserved QV in the case where there is no transmission in the continuous

¹Remark that causality in the center of the volatility distribution can be easily tested relying on the usual framework of Granger causality in mean applied to realized measures of volatility. As a will see in the sequel, for causality in the upper tail of the volatility distribution, one should first define the statistical meaning of extreme volatility.

(*IV*) component. For this, it suffices to choose in the first step a realized measure that is a consistent estimator of the integrated variance and another for the quadratic variance in a second step. Rejection of the null of no causality in the latter and no rejection in the former would indicate that the spillovers occur mainly through the jump channel. Extensive Monte Carlo simulations are subsequently conducted and the results show that our test has good finite sample size and power properties even in realistic samples.

The issue addressed in this paper, albeit seemingly related to the recent literature on causality in (extreme) quantiles (Hong et al., 2009; Jeong et al., 2012; Han et al., 2016), is not redundant. Indeed, Hong et al. (2009) introduce a testing approach for causality in downside risk to check for spillover effects in tail events for financial time series such as asset returns. Their methodology is well suited to detect causality in extreme conditional variance, since variance spikes induce large fluctuations in asset returns. In contrast, our paper focuses directly on volatility, which enables us to use realized measures of variance, i.e., model-free consistent estimators of the true latent process of variance. Second, the concept of cross-quantilogram introduced by Han et al. (2016) can be applied to realized volatility measures to check for causality in extreme variance, but it is built in an unconditional setup, while our conditional framework involves a state-dependent measure of extreme variance. Moreover, their test statistics has a non-standard asymptotic distribution. Lastly, in contrast to Jeong et al. (2012) who address the issue of causality in quantiles, our methodology goes beyond quantiles, as it looks at causality for exceedences, i.e., tail-events corresponding to occurrences of variance spikes that exceed extreme conditional quantiles (of the variance distribution).

The economic rationale of our testing approach relies on the economic content of asset volatility as evidenced by Christiansen et al. (2012).² The authors search for the drivers of financial volatility for multiple asset classes (equities, foreign exchange, bonds and commodities) by relying on a data-rich forecasting methodology and a Bayesian Model Averaging approach. They find, among others, that proxies for credit risk (the default spread as measured by the yield spread between BAA and AAA rated bonds) and funding market liquidity (the TED spread as measured by the difference between the 3-month LIBOR rate and T-Bill rate) are strong predictors of financial volatility. The predictive content of these factors is shown to be higher than the one conveyed by macroeconomic variables including inflation rate and industrial production. This stylized fact seems to indicate that periods of high volatility in financial assets are likely to coincide with high credit risk and tightened liquidity conditions. Hence, the transmission of high (or large) volatility across markets

²See also, Schwert (1989), Diebold and Yilmaz (2012), Paye (2012) and Cappiello et al. (2014).

can be viewed as the process of worldwide globalization of extreme credit and liquidity problems. This economic content of volatility transmission is important for regulators in quest of financial stability, and calls for an econometric tool to check for extreme volatility transmission across assets and markets.

We illustrate our causality test in extreme variance in an application on volatility transmission from the US equity market to six European markets. We find that the proposed test is able to identify the periods of large fluctuations in the US financial system that spillover to Europe and they are consistent with historical evidence. Our causality test in extreme volatility is also useful to check the hypothesis that spillovers in volatility are related to the volatility of macroeconomic variables (Hong, 2001; Cappiello et al., 2014). In the second part of the application we hence tackle the link between the presence of causality and the US monetary policy (through the shadow rate). We find that an increase in the causality measure can be indeed associated with the variability of the US shadow rates and implicitly instabilities in the monetary policy.

The rest of the paper is structured as follows. Section 2 introduces the null hypothesis of Granger non-causality and the unfeasible test-statistic of causality in extreme integrated variance. Section 3 details the steps of the feasible testing procedure and develops its asymptotic properties. In Section 4 we study the small-sample properties of the proposed testing procedure. An extension to the quadratic variance is considered in Section 5. An empirical illustration on extreme variance transmission in equity markets is further presented in Section 6. Section 7 concludes the paper, and all the proofs and mathematical derivations are gathered in Appendix A.

2 Hypothesis of interest and unfeasible test-statistic

In this section we discuss the concept of Granger causality in extreme variance under a general specification of the asset price process. We consider a frictionless arbitrage-free market in which the logarithm of the latent (efficient) price $p_i(\tau)$ of a given asset i at a continuous time τ , $\tau \in [t-1, t]$ with t a positive integer, is specified as a general semi-martingale process on the probability space (Ω, \mathcal{F}, P) where Ω represents the possible states of the world and \mathcal{F}_τ is the σ -field reflecting the information at time τ :

$$dp_i(\tau) = \mu_i(\tau)d\tau + \sigma_i(\tau)dW_i(\tau) + \xi_i(\tau)dN_i(\tau), \quad (1)$$

where the drift term $\mu_i(\tau)$ is a predictable process of locally bounded variation, $\sigma_i(\tau)$ is a *càdlàg* process bounded away from zero almost surely with $\int_{t-1}^t \sigma_i^2(\tau)d\tau < +\infty$, $\forall t > 0$, known as the instantaneous variance in absence of jumps, $W_i(\tau)$ is a standard Brownian

motion, and $J_i(\tau) = \xi_i(\tau)N_i(\tau)$ denotes a finite activity jump process. In particular, $N_i(\tau)$ is a counting process with finite instantaneous intensity λ_τ ($0 \leq \lambda_\tau < \infty$), and $\xi_i(\tau)$ is a non-zero random variable representing the jump in price with instantaneous mean of $\exp(\xi_i(\tau)) - 1$.

This specification is a very general representation of an asset return process that encompasses many continuous time models used in standard asset pricing theory, such as stochastic volatility models with possibly discontinuous sample paths (Todorov and Tauchen, 2011), models with leverage effects (Bollerslev et al., 2006), and models with time-varying dynamics for the jump process (Chan and Maheu, 2002).

The corresponding equispaced discrete-time intraday returns observed on the t^{th} trading day are given by

$$r_{i,t-1+j\Delta} = p_{i,t-1+j\Delta}^* - p_{i,t-1+(j-1)\Delta}^*, \quad (2)$$

$$p_{i,t-1+j\Delta}^* = p_{i,t-1+j\Delta} + \epsilon_{i,t-1+j\Delta}, \quad (3)$$

where $p_{i,t-1+j\Delta}^*$ are the observed prices and $\epsilon_{i,t-1+j\Delta}$ is the microstructure noise related to market frictions, $j = 1, 2, \dots, M$, M is the number of intraday returns over day t , and $\Delta = 1/M$ is the fixed sampling interval.

When $\sigma_i(\tau)$ is itself a stochastic process, a natural and general notion of return variability is the quadratic variation process over a fixed time period $[t-1, t]$, say one day. Under a general continuous time process as (1), this true ex-post measure of variance is given by

$$\begin{aligned} QV_{i,t} &= \int_{t-1}^t \sigma_i^2(\tau) d\tau + \sum_{t-1 < \tau < t} (J_i(\tau))^2 \\ &\equiv IV_{i,t} + JV_{i,t}, \end{aligned} \quad (4)$$

where the integrated variance $IV_{i,t}$ and the cumulative squared jump $JV_{i,t}$ measure the daily variance arising from the continuous and discontinuous parts of the log-price process, respectively. Without loss of generality, here the object of econometric interest is the integrated variance, but the main idea readily extends to the quadratic variation, and we defer this discussion to Section 5. Our aim is to develop an inferential procedure to check for the absence of transmission or causality between large (extreme) values of the integrated variance. We choose to focus on the quadratic variation of the continuous diffusive process as it has been shown to be the main channel of propagation of financial risk (see Corradi et al., 2012; Soucek and Todorova, 2014, among others) whereas comovements in jumps occur very seldom (see e.g. Jacod and Todorov, 2009; Bibinger and Winkelmann, 2015).

2.1 Granger causality in extreme variance

Let $IV_{1,t}$ and $IV_{2,t}$ be the processes of integrated variance for two financial assets. We denote by $F_{i,t}(\cdot)$, $i = \{1, 2\}$, the conditional cumulative distribution function of $IV_{i,t}$ and by $q_{i,t}(\alpha) \equiv F_{i,t}^{-1}(\alpha; \mathcal{F}_{t-1}^{(i)}) \equiv F_{i,t}^{-1}(\alpha)$ the conditional quantile of $IV_{i,t}$ for an α confidence level, which hence satisfies $P(IV_{i,t} > q_{i,t}(\alpha) | \mathcal{F}_{t-1}^{(i)}) = \alpha$, where $\mathcal{F}_{t-1}^{(i)} = \{IV_{i,t-H}, \dots, IV_{i,t-1}\}$ represents the information set available at time $t-1$ for the i^{th} asset, with H a user specified lag-order. Note that, without loss of generality, we discuss only the case of large values of α (for example $\alpha = 0.90, 0.95$) as we focus on the upper tail of the conditional distribution of $IV_{i,t}$ that is more relevant for volatility risk. In practice, α should be determined by regulators or market participants depending on their objective function or risk aversion level.

The null hypothesis of no Granger causality in extreme variance

$$\mathbb{H}_0 : P(IV_{1,t} > q_{1,t}(\alpha) | \mathcal{F}_{t-1}^{(1)}) = P(IV_{1,t} > q_{1,t}(\alpha) | \mathcal{F}_{t-1}), \quad (5)$$

with $\mathcal{F}_{t-1} = (\mathcal{F}_{t-1}^{(1)}, \mathcal{F}_{t-1}^{(2)})$ the joint information set available at time $t-1$, states that $IV_{2,t}$ does not Granger cause $IV_{1,t}$ in its conditional extreme quantile of order α . Put differently, information about extreme variance in the second asset, i.e. $IV_{2,t}$ goes beyond its conditional quantile, is not useful to predict the occurrence of a future extreme variance in the first asset.

To reformulate (5) in terms of no Granger causality in mean, let us transform the integrated variance process $IV_{i,t}$ into an exceedance (extreme variance) indicator

$$z_{i,t}(\alpha) = \begin{cases} 1 & \text{if } IV_{i,t} \geq q_{i,t}(\alpha) \\ 0 & \text{otherwise.} \end{cases} \quad (6)$$

The null hypothesis of absence of causality in extreme variance from the second asset to the first is then equivalently expressed as

$$\mathbb{H}_0 : \mathbb{E} \left(z_{1,t}(\alpha) \middle| \mathcal{G}_{t-1}^{(1)} \right) = \mathbb{E} (z_{1,t}(\alpha) | \mathcal{G}_{t-1}), \quad (7)$$

where $\mathcal{G}_{t-1} = \{\mathcal{G}_{t-1}^{(1)}, \mathcal{G}_{t-1}^{(2)}\}$ and $\mathcal{G}_{t-1}^{(i)} = \{z_{i,t-H}, \dots, z_{i,t-1}\}$ is the information set available at time $t-1$ for the i^{th} asset.³

Notice that $z_{1,t}$ is an i.i.d. Bernoulli sequence since it is defined as a conditional quantile-exception process. We exploit this information in the following subsection and propose a Portmanteau-type statistic for the Granger causality in extreme variance hypothesis.

³A more general setup would be to define the information set $\mathcal{G}_{t-1}^{(i)}$ as $\mathcal{G}_{t-1}^{(i)} = \{z_{i,1}, \dots, z_{i,t-1}\}$, hence developing a test that is consistent against causality for all possible lags. We do not follow this alternative for two reasons. First, it is expected that causality in extreme variance is a short-lived phenomenon in financial markets, which should materialize in a few days. Second, considering the case with $H \rightarrow \infty$ would complicate the asymptotic analysis.

2.2 Infeasible test-statistic

We now propose a test-statistic for (7). For this, we draw upon the univariate Portmanteau test statistics in Ljung and Box (1978) and exploit the cross-correlation structure of the exceedance indicators associated with the extreme variance events in the two assets considered. Suppose that $IV_{i,t}$ and $q_{i,t}(\alpha)$ are observable. Then we can construct the corresponding exceedance indicators $z_{i,t}(\alpha)$ and define their cross-lagged covariance of order j by

$$C(j) = \begin{cases} T^{-1} \sum_{t=1+j}^T (z_{1,t}(\alpha) - \pi)(z_{2,t-j}(\alpha) - \pi), & 0 \leq j \leq T-1 \\ T^{-1} \sum_{t=1-j}^T (z_{1,t+j}(\alpha) - \pi)(z_{2,t}(\alpha) - \pi), & 1-T \leq j \leq 0, \end{cases}$$

where $\pi = 1 - \alpha$ is the expected value of the indicator variables. The cross-correlation function between $z_{1,t}(\alpha)$ and $z_{2,t}(\alpha)$ is defined as

$$\rho^*(j) = \frac{C(j)}{\pi(1-\pi)}. \quad (8)$$

It follows that the test-statistic $Q^*(H)$ for a fixed number of lags H takes the form

$$Q^*(H) = T(T+2) \sum_{h=1}^H \frac{\rho^{*2}(h)}{T-h}. \quad (9)$$

3 Feasible test statistics and asymptotic theory

The test-statistic in (9) is valid only under the assumption that $IV_{i,t}$ and $q_{i,t}(\alpha)$ are observable. However, in practice, the integrated variance and its conditional quantile are latent and must be estimated. In this section we discuss their estimation, define the feasible test-statistic and tackle the impact of estimation uncertainty on the limit distribution of the feasible test-statistic.

3.1 IV estimation

Since the integrated variance is not directly observable, any inferential procedure should be based on suitable estimators of this quantity. A number of parametric and non-parametric estimators of $IV_{i,t}$ are available in the literature. We choose to focus on non parametric procedures so as to avoid any specific functional form assumptions about the stochastic process(es) governing the local martingale and the drift process. They produce asymptotically unbiased variance measures under quite general conditions. In particular, we rely on the very rich literature on realized variance measures (see among others Andersen et al., 2003; Barndorff-Nielsen and Shephard, 2004; Hansen and Lunde, 2006; McAleer and Medeiros,

2008b; Barndorff-Nielsen et al., 2008; Andersen and Benzoni, 2009) and compute ex-post estimates of variance by effectively exploiting the information inherent in observed high-frequency intradaily data.

Two main questions generally arise when using realized measures: i) is the microstructure noise corrected and ii) how are jumps handled? Since we focus on causality in the integrated variance of the price process, we tackle the second issue simply by considering jump-robust realized variance measures, that have been shown to be consistent estimators of the IV . At the same time, microstructure noise arises from many sources including asynchronous trading, liquidity effects, bid/ask bounce, misrecordings, or price discreteness and it can induce serial auto-correlation in intradaily data and / or prevalent zero returns. As a consequence, the estimate of the integrated variation can be biased at high sampling frequencies. Although jump-robust realized variances are generally not robust to noise (e.g. the bipower variation of (Barndorff-Nielsen and Shephard, 2004), that is still the most popular jump-robust realized variance measure), estimators of $IV_{i,t}$ that attenuate or are robust to microstructure noise have been proposed in the literature and include the median realized variance in Andersen et al. (2012) and the quantile-based realized variance in Christensen et al. (2010).

All these realized estimators of variance share the fundamental property that they have been shown to consistently estimate the integrated variance as the number of intradaily observations increases

$$IV_{i,t,M} \xrightarrow[M \rightarrow \infty]{p} IV_{i,t}, \quad (10)$$

where $IV_{i,t,M}$, $t = 1, \dots, T$ denotes a given daily realized measure of integrated variance based on M intradaily returns. Consequently, robust to microstructure noise or not, they are all natural candidates to approximate the latent process of integrated variance when one focuses on the problem of testing for causality in extreme $IV_{i,t}$.

3.2 Conditional quantile estimation

The last ingredient needed to construct the feasible causality test in extreme integrated variance is a model for the dynamics of $IV_{i,t,M}$ in their upper conditional distribution tail. To this aim, we propose to rely on a semiparametric approach, namely the heterogeneous autoregressive quantile model (HARQ) of Zikes and Barunik (2014). Let $q_{i,t,M}(\alpha; \theta_i)$ be the conditional quantile of $IV_{i,t,M}$ for a confidence level α , where θ_i is a finite dimensional vector of parameters. The HARQ model writes

$$q_{i,t,M}(\alpha; \theta_i) = \theta_{i,1}(\alpha) + \theta_{i,2}(\alpha)IV_{i,t-1,M} + \theta_{i,3}(\alpha)V_{i,t-1:t-5,M} + \theta_{i,4}(\alpha)V_{i,t-1:t-22,M}, \quad (11)$$

with $\theta_i = \theta_i(\alpha)$ the vector of unknown parameters, and

$$V_{i,t-1:t-L,M} = \frac{1}{L} \sum_{l=1}^L IV_{i,t-l,M}. \quad (12)$$

Equation (11) can be viewed as an adaptation to the quantile regression framework of the heterogeneous autoregressive (HAR) model of Corsi (2009) as it relates the quantile of a given realized measure of integrated variance to the values of the latter averaged over different time horizons (daily, weekly and monthly). We make the following assumption about the dynamics of $q_{i,t}(\alpha)$, the true quantile of the integrated variance process $IV_{i,t}$,

Assumption 1 *There exists a unique parameter set $\theta_i^0 = \theta_i^0(\alpha)$ such that*

$$q_{i,t}(\alpha) = \theta_{i,1}^0 + \theta_{i,2}^0 IV_{i,t-1} + \theta_{i,3}^0 V_{i,t-1:t-5} + \theta_{i,4}^0 V_{i,t-1:t-22}, \quad (13)$$

with

$$V_{i,t-1:t-L} = \frac{1}{L} \sum_{l=1}^L IV_{i,t-l}, \quad l \in \{5, 22\}. \quad (14)$$

Assumption 1 rules out misspecification as it assumes that the integrated variance and its realized measure have the same tail dynamics. One can wonder whether this assumption holds. In fact, this is only a weak assumption, that can be motivated by the high persistence of daily volatility that is observed empirically. Indeed, the general data generating process in (1) is compatible in some cases with an ARMA representation for the integrated variance (Meddahi, 2003), and hence with an infinite-order AR representation if the process is invertible. Subsequently, the infinite order AR process can be well approximated by a finite-lag long-memory AR model, like the HAR (see Corsi, 2009). By analogy, the HARQ model appears to be appropriate when focusing explicitly on tail dynamics (see Zikes and Barunik, 2014). Most importantly, the HARQ model shows the ability to reproduce this stylized fact and appears to be a simple and elegant way to accurately estimate and forecast conditional quantiles for realized measures of variance.

The parameters of the HARQ model are easily estimated by minimizing the “tick” loss function of Koenker and Bassett Jr (1978), *i.e.*,

$$\hat{\theta}_i = \arg \min_{\theta_i} \frac{1}{T} \sum_{t=2}^T [\alpha - \mathbb{I}(u_{i,t} < 0)] u_{i,t}, \quad (15)$$

$$u_{i,t} = IV_{i,t,M} - q_{i,t,M}(\alpha; \theta_i), \quad (16)$$

with T the sample size and $\mathbb{I}(\cdot)$ the usual indicator function. The estimation of the quantile regression in (11) complicates the derivation of the limit distribution of the causality test. We discuss this issue in Subsection 3.4 and show that the impact of parameter estimation uncertainty vanishes asymptotically.

3.3 Feasible test-statistic

To construct the feasible test-statistic we replace the unknown $IV_{i,t}$ and $q_{i,t}$ sequences in (9) with their estimated counterparts, the realized measures $IV_{i,t,M}$ and the estimated quantiles $q_{i,t,M}(\alpha; \hat{\theta}_i)$. It follows that the feasible Granger-causality in extreme variance test-statistic for a fixed number of lags H is

$$\hat{Q}(H) = T(T+2) \sum_{h=1}^H \frac{\hat{\rho}^2(h)}{T-h}, \quad (17)$$

where $\hat{\rho}$ is the sample cross-lagged correlation function associated with the observed exceedance indicators $z_{1,t,M}(\alpha; \hat{\theta}_1)$ and $z_{2,t,M}(\alpha; \hat{\theta}_2)$.

Our testing procedure is semiparametric in nature, as it uses the information extracted from the observed high-frequency intradaily returns to construct the nonparametric estimators for the latent integrated variance process and a simple semiparametric quantile regression to estimate the conditional quantile of the realized variance process. It is simple to implement and intuitive and it can be applied to any type of financial assets that is liquid enough so as to observe intradaily prices at a reasonable high frequency (e.g. every 1 or 5 minutes) that would insure good realized variance estimates in finite samples. Naturally, any consistent (realized) measure of integrated variance can be considered. This generality is asymptotically justified by the robustness of our test-statistic to microstructure noise (see Subsection 3.4).

3.4 Asymptotic theory

We now derive the limit distribution of the feasible causality test in extreme variance under the null hypothesis. Given that the true $IV_{i,t}$ and $q_{i,t}$ are unobservable and hence estimated, deviations of $\hat{Q}(H)$ from $Q(H)$ or equivalently differences between $z_{i,t,M}(\alpha; \hat{\theta}_i)$ and $z_{i,t}(\alpha; \theta_i)$ may occur for two reasons. They can arise first from the approximation of the integrated variance $IV_{i,t}$ by $IV_{i,t,M}$, and second from the estimation of the quantile regression (11). We provide some regularity conditions on the continuous time process and the conditional quantiles of the realized measures and then show that under these mild assumptions, our test statistic for causality in extreme variance has an asymptotic distribution which is free of these two sources of estimation risk.

Assumption 2 *The drift term of the logarithmic price process in (1) is locally bounded with $\mathbb{E} |\mu_{i,t}|^{2k} < \infty$, the diffusive function is càdlàg with $\mathbb{E} |\sigma_{i,t}|^{2k} < \infty$, and the jump sizes $\xi_i(t)$ are i.i.d. with $\mathbb{E} |\xi_i(t)|^{2k} < \infty$, for some $k \geq 2$. The microstructure noise is i.i.d. with symmetric distribution around zero and has finite $2k^{\text{th}}$ moment for some $k \geq 2$.*

Assumption 3 Let $\mathcal{G}_{i,t} = \{IV_{i,s,M}, s \leq t\}$ be the information set available at time t for the realized measure $IV_{i,t,M}$, $i \in \{1, 2\}$, and Θ_i a compact set where the vector of parameters θ_i lies. The quantile $q_{i,t,M}(\alpha; \theta_i)$ is differentiable in Θ_i and for all θ_i in a neighborhood of θ_i^0 , the true unknown vector of parameters, such that $\|\theta_i - \theta_i^0\| \leq d$ for d sufficiently small, $\|\nabla q_{i,t,M}(\alpha; \theta_i)\| \leq K(\mathcal{G}_{i,t})$, where $K(\mathcal{G}_{i,t})$ is some stochastic function of the variables that belongs to $\mathcal{G}_{i,t}$ and $\mathbb{E}[K(\mathcal{G}_{i,t})^3] \leq K_0 < \infty$ for some constant K_0 .

Assumption 4 $\max\{g_{i,t}(\varepsilon), g_{12,t}(\nu, \xi)\} \leq U < \infty \forall t$, where $g_{i,t}(\varepsilon)$ is the conditional density of $IV_{i,t,M} - q_{i,t,M}(\alpha; \theta_i^0)$, $i \in \{1, 2\}$, and $g_{12,t}(\nu, \xi)$ is the bivariate joint conditional density of $(IV_{1,t,M} - q_{1,t,M}(\alpha; \theta_1^0), IV_{2,t,M} - q_{2,t,M}(\alpha; \theta_2^0))$.

Assumption 2 corresponds to Assumption 6 in Corradi et al. (2012). These conditions help them to bound the integrated variance estimation error, $N_{i,t,M} = IV_{i,t} - IV_{i,t,M}$, by establishing the existence of a sequence b_M with $b_M \rightarrow \infty$ as $M \rightarrow \infty$, such that $\mathbb{E}|N_{i,t,M}|^k = O(b_M^{-k/2})$ for some $k \geq 2$. Hence, under Assumption 1, the k^{th} moment of the absolute estimation error that arises from approximating the integrated variance $IV_{i,t}$ by $IV_{i,t,M}$ is bounded. For example, $b_M = M$ when the integrated variance is approximated by the realized bi(tri)power variation.

Assumptions 3 and 4 are regulatory conditions about the assumed dynamics of the quantiles of the realized measures of variance. They allow us to contain parameter estimation uncertainty in the HARQ model (see also assumptions AN1(a) and AN2(a) in Cappiello et al., 2014). In particular, we are able to bound the expected value of the error from approximating the exceedance indicators $z_{i,t,M}(\alpha; \theta_i)$ by their sample estimates, $z_{i,t,M}(\alpha; \hat{\theta}_i)$. We now establish the asymptotic distribution of $\hat{Q}(H)$.⁴

Proposition 1 *Let Assumptions 2-4 hold. Under the null hypothesis of absence of causality in extreme variance as stated in (7), if $T^{\frac{1}{k-1}} b_M^{-1/2} \rightarrow 0$, as $T, M \rightarrow \infty$, we have*

$$\hat{Q}(H) \sim \chi_H^2, \quad (18)$$

where χ_H^2 is the chi-square distribution with H degrees of freedom.

The proposition shows that it suffices that M grows faster than a power of T (or simply $M \rightarrow \infty$ regardless of T 's rate of convergence if all moments exist, i.e. $k = \infty$) for the contribution of the measurement error to vanish asymptotically and the feasible test-statistic

⁴Another way to construct a causality test in extreme variance would have been based on continuous quantile exceedance variables, $IV_{i,t,M} \times z_{i,t,M}(\alpha; \hat{\theta}_i)$. However, these variables are expected to be heteroskedastic and the limit distribution of the test should no longer be the standard χ^2 distribution. One advantage of our current framework is that the test is easy to implement and its asymptotic properties are simple to derive.

to be χ^2 distributed. The proof of Proposition 1 is based on the following decomposition of our test-statistic

$$\widehat{Q}(H) = Q^*(H) + (\widehat{Q}(H) - Q(H)) + (Q(H) - Q^*(H)), \quad (19)$$

where $Q^*(H)$ is the infeasible test statistic defined in (9), that is based on the true unknown integrated variance processes $IV_{i,t}$ and their true conditional quantiles. At the same time, $Q(H)$ corresponds to another infeasible test statistic that is based on the realized measure $IV_{i,t,M}$ and its true quantile $q_{i,t,M}(\alpha; \theta_i^0)$. In other words, $Q(H)$ supposes that the HARQ model is estimated without error such that the test-statistic can be formed as if the true parameters θ_i^0 were known and were equal to their estimates $\hat{\theta}_i$. The following three Lemmas provide a sketch of the proof (see Appendix A for a full proof).

Lemma 1 *Under the null hypothesis of absence of causality in extreme variance, as $T \rightarrow \infty$,*

$$Q^*(H) \sim \chi_H^2, \quad (20)$$

where χ_H^2 is, as expected, the chi-square random variable with H degrees of freedom.

Lemma 2 *Under Assumptions 3 and 4, as $T \rightarrow \infty$,*

$$\widehat{Q}(H) - Q(H) = o_p(1). \quad (21)$$

Lemma 3 *Under Assumption 2 and 3, if $T^{\frac{1}{k-1}} b_M^{-1/2} \rightarrow 0$, as $T, M \rightarrow \infty$,*

$$Q(H) - Q^*(H) = o_p(1). \quad (22)$$

Lemma 1 establishes the asymptotic distribution of the infeasible test statistic $Q^*(H)$, which turns out to be the same as the one of the feasible test statistic $\widehat{Q}(H)$. This equivalence in terms of asymptotic distribution holds because estimation error vanishes or it is bounded asymptotically. Lemma 2 shows that this is the case for the error arising from the estimation of the HARQ model, and Lemma 3 confirms the boundedness of the error arising from approximating the true integrated variance process $IV_{i,t}$ by its realized counterpart $IV_{i,t,M}$. Consequently, the proposed test for Granger causality in extreme variance is easy to compute and also to interpret as it has a standard asymptotic distribution.

4 Finite sample properties

This section is devoted to the analysis of the finite sample properties of our causality test. We tackle the size properties in the first part of the section, while the second part focuses on the power analysis.

4.1 The size of the test

For each asset $i \in \{1, 2\}$, we follow Aït-Sahalia and Mancini (2008) and simulate the process of efficient log-returns as $r_{i,t+j\Delta} = r_{i,t+j\Delta}^{(c)} + r_{i,t+j\Delta}^{(d)}$, with $j = 1, 2, \dots, M_0$, $\Delta = 1/M_0$, and where $M_0 = 23,400$ is the number of intraday returns for a 1 second sampling frequency and a trading day of 6.5 hours. The corresponding process of efficient log-prices $p_{i,t+j\Delta}$ is obtained by assuming an initial value equal to $\log(100)$ such that the observed log-price process is equal to $p_{i,t+j\Delta}^* = p_{i,t+j\Delta} + \epsilon_{i,t+j\Delta}$, with $\epsilon_{i,t+j\Delta}$ the i.i.d.N microstructure noise with mean $\mu_{\epsilon_i} = 0$ and standard deviation $\sigma_{\epsilon_i} = 0.1\%$.

The continuous part of the intraday log-returns is given by

$$r_{i,t+j\Delta}^{(c)} = \sqrt{IV_{i,t+1}} v_{i,t+j\Delta}, \text{ for } i \in \{1, 2\} \quad (23)$$

with $v_{i,t+j\Delta}$ two independent Gaussian strong white noise processes with mean 0 and variance $\sigma_{v_{i,t+j\Delta}}^2 = 1/M_0$, and $IV_{i,t+1}$ the daily integrated variances. The dynamics of $IV_{i,t+1}$ is specified as in McAleer and Medeiros (2008a) so as to entail a realistic asset price process. Relevant stylized facts in volatility dynamics such as long-range dependence, non-stationarity, non-normality, presence of clusters of volatility are taken into account (see Figure 1). In particular, each log-volatility follows a stationary three-regime smooth-transition heterogeneous autoregressive (HARST) model

$$IV_{i,t} = \exp(\sigma_{i,t}^2), \quad (24)$$

$$\sigma_{i,t} = \beta_0' y_{i,t} + \sum_{m=1}^2 \beta_m' y_{i,t} f(r_{i,t-1}^{(22)}, \gamma_m, c_m) + \varepsilon_{i,t},$$

where $y_t = (1, \sigma_{i,t-1}, \sigma_{i,t-1:t-5}, \sigma_{i,t-1:t-22})$, with $\sigma_{i,t-1:t-L} = L^{-1} \sum_{l=1}^L \sigma_{i,t-l}$, and where the innovations $\varepsilon_{i,t}$ are independent Gaussian strong white noises of variance $\sigma_{\varepsilon_i}^2 = 0.25^2$. Besides, $f(r_{i,t-1}^{(22)}, \gamma_m, c_m)$ is the logistic transition function with the transition variable $r_{i,t-1}^{(22)}$ given by the cumulative daily closing return over the last month. $\gamma_1 = \gamma_2 = 4$ are the slope parameters of $f(\cdot)$, whereas $c_1 = -10$ and $c_2 = 13$ are its threshold parameters. $\beta_0 = (0.01, 0.95, 0, 0)$ corresponds to the background persistent first-order autoregressive dynamics of the log-volatility process which can be labeled as the turbulent regime, for which $f(r_{i,t-1}^{(22)}, \gamma_m, c_m) \approx 0$, with $m \in \{1, 2\}$. At the same time, $\beta_1 = (-0.35, -0.58, 0.27, 0.21)$

allows the process to rapidly recover after periods of very negative returns, i.e. $r_{t-1}^{(22)} < c_1$, such that $\sigma_{i,t} \approx (\beta_0 + \beta_1)'y_{i,t} + \varepsilon_{i,t}$ correspond to the calm regime, with $f(r_{i,t-1}^{(22)}, \gamma_1, c_1) \approx 1$ and $f(r_{i,t-1}^{(22)}, \gamma_2, c_2) \approx 0$. Finally, $\beta_2 = (0.03, 0.3, -0.2, -0.18)$ corresponds to the case where returns are very positive, i.e. $r_{t-1}^{(22)} > c_2$. Hence, $\sigma_{i,t} \approx (\beta_0 + \beta_1 + \beta_2)'y_{i,t} + \varepsilon_{i,t}$ give the dynamics of log-volatility in a secondary turbulent regime, with $f(r_{i,t-1}^{(22)}, \gamma_m, c_m) \approx 1$.

The discontinuous jump component of the efficient log-returns process $r_{i,t+j\Delta}^{(d)}$ is defined as a Poisson-type (finite-activity) jump process

$$r_{i,t+j\Delta}^{(d)} = c_{i,t+j\Delta} \mathbb{I} \left(U(0, 1) < \frac{\lambda_i}{M_0} \right), \quad (25)$$

where the jump size $c_{i,t+j\Delta}$ is assumed to be normally distributed with mean $\mu_{c_i} = -0.01\%$ and standard deviation $\sigma_{c_i} = 1$, $\mathbb{I}(\cdot)$ is an indicator function, $U(0, 1)$ is the uniform distribution over $[0, 1]$, and $\lambda_i = 0.5$, which implies on average a jump every two days.

Under the null hypothesis there is no causality in extreme volatility from $IV_{2,t}$ to $IV_{1,t}$ with respect to \mathcal{F}_{t-1} . We hence examine the size of our test in finite samples by generating from the above DGP independent sequences of $M_0 = 23,400$ 1-second intradaily high-frequency log-returns for each of the two financial assets and for each day $t = 1, \dots, T$ in the sample, where $T \in \{500; 1,000; 2,000\}$, i.e. two to eight years of daily data. The daily integrated variance $IV_{i,t}$ is subsequently estimated by the bipower variation,

$$BV_{i,t,M} = \frac{\pi}{2} \sum_{j=2}^M |r_{i,t+j\Delta}| |r_{i,t+(j-1)\Delta}| \quad (26)$$

based on M equally spaced intraday returns. As the sampling frequency M decreases, the microstructure market effects diminish but the realized measure is less accurate as it is based on fewer observations. Therefore, in the simulations design we set $M \in \{390; 78; 26; 13\}$ that corresponds to a sampling frequency of 1, 5, 15 and 30 minutes, respectively. Without loss of generality, we examine the size of the test for two quantile levels, $\alpha \in \{0.9; 0.95\}$, in the upper right tail of the variance process and we set the maximum lag-order $H \in \{3; 5; 10\}$.⁵

Table 1 in Appendix B displays the empirical size of the Granger-causality test in extreme volatility for a given value of the quadruplet (α, H, T, M) . The results are based on 1,000 simulations. The nominal significance level of the test is set to $\eta = 5\%$. Overall we find that the causality test in extreme variance is adequately sized, i.e. the rejection frequencies are close to the retained significance level. The asymptotic chi-square distribution thus provides a good approximation for the finite-sample distribution of our test statistic. The choice of

⁵A rule of thumb for the choice of the maximum lag order in Portmanteau test-statistics has been proposed by RJ Hindman, who suggests the use of $H = 10$. This choice seems reasonable for the financial markets, where news is generally integrated very fast in the decisions taken by market participants.

M and H appears to have a rather limited impact on the size of the test for a given quantile α and sample size T .

In the spirit of a robustness check analysis, the finite-sample properties of our test are also investigated by relying on a jump-robust realized measure that also attenuates the effect of microstructure noise, which is the median realized variance of Andersen et al. (2012) :

$$medRV_{i,t,M} = \frac{\pi}{6 - 4\sqrt{3} + \pi} \left(\frac{M}{M-2} \right) \sum_{j=2}^{M-1} \text{med}(|r_{i,t+(j-1)\Delta}|, |r_{i,t+j\Delta}|, |r_{i,t+(j+1)\Delta}|)^2.$$

We find that the size of the test is not influenced by choice of the realized measure of variance since the rejection frequencies are strictly identical to those obtained with the BV measure.

4.2 The power of the test

To analyze the empirical power, we simulate the intradaily data for the second time series by assuming the data generating process (DGP) described above. In contrast, we modify the DGP of the first series such that the dynamics of the daily integrated process in (24) incorporates causality in volatility under the alternative hypothesis (e.g. see Figure 2). In particular, we consider that

$$IV_{1,t} = \exp(\sigma_{1,t}^2), \tag{27}$$

$$\sigma_{1,t} = \gamma \sigma_{2,t-1:t-J} + \delta \left(\beta'_0 y_{1,t} + \sum_{m=1}^2 \beta'_m y_{1,t} f(r_{1,t-1}^{(22)}, \gamma_m, c_m) \right) + \varepsilon_{1,t}, \tag{28}$$

with γ and δ positive parameters. Note that with $\gamma = 0$ and $\delta = 1$ the DGP simplifies to the framework considered in the size analysis. We set δ to 0.5 in order to keep the two daily log-volatility series on reasonable scales. Besides, we fix J to 5 as it seems natural to assume that the recent past extreme events in the variance of an asset (within the previous week) influence the occurrence of extreme events in the variance of another asset, whereas the impact of remote events, say a month before, can be assumed to be negligible. Note that in (28) we introduce dependence in the whole distribution of the log-volatilities instead of only in the conditional upper quantile. This has minor consequences for the power of the test as causality is implicitly present in the extreme right tail of the variance, but it allows us to keep the already complex DGP reasonable. We use different values for the intensity of causality by setting the γ parameter to 0.5 and 0.8, respectively. The larger γ , the stronger the causality of $\sigma_{2,t}$ for $\sigma_{1,t}$.

Tables 2 and 3 in Appendix B display the rejection frequencies over 1,000 simulations for $\gamma = 0.5$ and $J = 5$ in the case of the BV and $medRV$ measures, respectively. The results indicate that our test of causality in extreme variance has appealing power properties

irrespective of the realized measure considered. The larger T is, for the same α , H and M , the better the power is. The optimal number of lags in the Portmanteau statistic corresponds to the true dependence horizon, J , used in the DGP. The power results also suggest that in an empirical application where the true J is unknown it is preferable to overestimate the number of lags rather than to underestimate it. Overall, we observe two distinct patterns. First, for a given value of α , the empirical power decreases when both M and T decrease. This result is expected, because an accurate approximation of the daily latent process of integrated variance requires sampling intradaily data at high frequencies ($M \rightarrow M_0$). Moreover, one needs a large sample of daily observations ($T \rightarrow \infty$) for the Ljung-Box test statistics to accurately capture causality in daily variance (and register a power close to 1). Second, for a given value of the triplet (H, T, M) the empirical power decreases when the tail-risk level $1 - \alpha$ decreases. This result is also expected and arises from the low number of tail-events between which causality is tested. To give more insight about the power properties of our new test, we report in Tables 4 and 5 the empirical power obtained when the parameter γ is set to 0.8 for each of the two realized measures. In all configurations, the higher γ , the stronger the causality from $\sigma_{2,t}$ to $\sigma_{1,t}$, which is confirmed by the larger power values relatively to those displayed in Tables 2 and 3 (for $\gamma = 0.5$).

5 Causality testing in quadratic variation

Our causality test in extreme variance in (17) can be easily extended to define the concept of causality in quadratic variation. This setting is general enough to allow not only for microstructure noise but also jumps in the continuous time variance process. In practice it is expected that jumps contain only few predictive information about the future level of volatility in its conditional tail, but we argue that the use of the proposed causality test both on IV and QV may help disentangle the sources of extreme volatility spillover in empirical applications. The null hypothesis in (5) becomes

$$\mathbb{H}_0 : P(QV_{1,t} > q_{1,t} | \mathcal{F}_{t-1}^{(1)}) = P(QV_{1,t} > q_{1,t} | \mathcal{F}_{t-1}),$$

or equivalently

$$\mathbb{H}_0 : \mathbb{E} \left(z_{1,t}(\alpha) \mid \mathcal{F}_{t-1}^{(1)} \right) = \mathbb{E} (z_{1,t}(\alpha) | \mathcal{F}_{t-1}),$$

where the exceedance indicators $z_{i,t}(\alpha)$ take the value 1 if $QV_{i,t}$ goes beyond its conditional quantile.

The feasible test procedure now relies in the first step on consistent (realized) estimators of the quadratic variation of a price process. The 5-min realized variance (RV) is the most

commonly used realized measure in the literature, but robust estimators that allow for the use of higher intraday sampling frequencies as the sub-sampled, two-scales, kernel, pre-averaged RV can also be considered. The conditional quantile of the realized measure of quadratic variation can be subsequently modelled by a HARQ specification analog to the one discussed in Section 3.2.

A key point in the development of this extension is to prove that the asymptotic theory in Section 3.4 still holds and hence our (feasible) causality test in quadratic variation is χ^2 distributed. For this, Assumptions 3 and 4 can be easily restated in terms of $QV_{i,t}$ and a new regularity condition, with respect to the jump process, is introduced:

Assumption 5 *The intensity of the Poisson counting process λ_τ is strictly stationary and the jump size satisfies the moments existence condition $\mathbb{E}|\xi_i(\tau)|^{2k} < \infty$ for some $k \geq 2$.*

Under this assumption it can be shown that the k^{th} moment of the estimation error on the discontinuous part of the model decays to zero at a fast enough rate, $\mathbb{E} \left| N_{i,t,M}^{(d)} \right|^k = O(b_M^{-k/2})$ for some $k \geq 2$, where $N_{i,t,M}^{(d)} = JV_{i,t,M} - JV_{i,t}$ (see Zikes and Barunik, 2014, for a more thorough discussion). It follows by the same arguments as in Proposition 1 that the feasible test-statistic has the same χ^2 limit distribution as the unfeasible one, i.e. estimation uncertainty does not impact the limit distribution of our test-statistic when it is used to check for Granger causality in extreme quadratic variation either.

5.1 Finite-sample properties

To study the finite sample properties of our causality test in the case of the quadratic variation we modify the DGP used in Section 4 so as to facilitate the introduction of causality in the jump process under the alternative hypothesis. To be more precise, we keep the definition of the continuous part of the intraday log-returns in (23) and (24) but we make the hypothesis that there is at most one jump per day and it occurs at a random time within the day. Indeed, the discontinuous Poisson-type jump component is generated at the daily level and reshaped into 1 second sampling frequency by drawing the intraday jump time from an uniform distribution. We set $\lambda_i = 0.25$ which is equivalent to an average rate of occurrence of a jump every four days. Besides, the jump size is assumed to be normally distributed with mean $\mu_{c_i} = -0.01\%$ and standard deviation $\sigma_{c_i} = 2$.

The daily quadratic variation, $QV_{i,t}$, is subsequently estimated by the realized kernel,

$$RK_{i,t,m} = \sum_{h=-H}^H \mathcal{K}\left(\frac{h}{H+1}\right) \gamma_h, \quad (29)$$

with $\gamma_h = \sum_{j=|h|+1}^M r_{i,t+j\Delta} r_{i,t+(j-|h|)\Delta}$, and $\mathcal{K}(\cdot)$ a Parzen kernel weight function, based on M equally spaced intraday returns.⁶

The finite sample size results based on 1000 replications are reported in Table 6. We observe a quite accurate approximation of the nominal level (set to $\eta = 5\%$) irrespective of the quadruplet (α, H, T, M) . The additional estimation steps from estimating the latent quadratic variations or their conditional quantiles do not significantly influence the finite sample properties of the test. These results go along the lines of our findings for the causality test in integrated variance.

To investigate the finite sample power properties of the test, we simulate the price process under two different alternative hypotheses. We first allow for extreme variance transmission through both the continuous and jump components and then we suppose that spillovers go only through the discontinuous jump channel. This analysis is expected to shade some light on the ability of our test to distinguish between the two sources of extreme variance transmission in small samples.

The *IV* spillovers are generated by setting $\gamma = 0.5$ in (28), see Section 4. As for the jump component, we draw the sizes of the jump processes from a multivariate normal distribution with identical means, μ_c , and variances, σ_c , (as in the size analysis) and correlation equal to 0.8. We then construct the two sequences of daily jump series by supposing that a jump in the second asset will transmit to the first asset in the following day at a randomly drawn intraday time. From an empirical perspective this is a quite mild assumption, as jumps are generally believed to spillover fast when they do transmit to other assets / markets. Note that we do not focus here on intraday transmission of extreme volatility, in which case the hypothesis of spillovers in jumps (within the day) would be even more realistic.⁷ Still, our test can be used on intradaily data as long as the user makes sure the assets / markets are liquid enough to construct consistent realized measures of variance on intradaily subintervals. Conversely, a user interested in extreme variance transmission at lower frequencies than the daily one could also implement our test, and in this case we recommend her the test for causality in *IV*.

Table 7 reports the power results under the first alternative hypothesis, i.e. when the source of causality is double. The test has good power properties against this alternative, and it becomes more powerful as M and T increase and α decreases. $H = 3$ appears to be the optimal lag length, that is justified by the fact that although spillovers in *IV* are

⁶A robustness check analysis based on the realized variance has been performed and it supports the findings obtained with $RK_{i,t,m}$ that are detailed below (these tables are available upon request).

⁷Co-jumps, i.e. jumps that occur at the same time on different assets / markets, have become a topical issue in financial econometrics, but their study is out of the scope of the paper. See, for example, Gnabo et al. (2014) for a recent test to identify co-jumps.

observed over the following week, jumps transmit only from one day to another.

In this rich setting, we can also investigate the power of our causality test in integrated variance under the alternative hypothesis of causality in both the continuous and discontinuous components of the quadratic variation. In Table 8 we report the results when IV is estimated by the bipower variation. The test appears to have slightly better power properties than that in Table 2 but its power remains relatively low in small samples of up to 1000 observations. In contrast, the causality test in quadratic variation (see Table 7) has much better power properties under this alternative hypothesis of double causality.

Table 9 reports the power of the test under the second alternative hypothesis, i.e. of causality only in the jump process. The test appears to exhibit good power properties, similar to those observed in the case of double causality (see Table 7). The only notable difference between the two is that now the lower H the better, i.e. the power improves as we get closer to the lead of one day at which we assumed that jumps spillover in the DGP.

As a by-product in this framework, we can investigate the size of the causality test in integrated variance when jump transmission is allowed for. The rejection frequencies are reported in Table 10. The test is well-sized when the sampling frequency is high ($M \geq 78$), but it tends to overreject at low frequencies. One reason behind this may be that a lower number of intraday returns is not able to fully compensate for the impact of a large jump and hence in some cases the causality in jumps may drive the test result.

6 Empirical Application

This section illustrates our causality testing procedure in an application on extreme volatility transmission between US and European Financial markets. We test in a first step for the presence of causality from the US equity market to several European equity markets over the period from January 4, 2000 to September 23, 2016. To this end, we use the bipower variation realized measure of variance defined in (26). In a second step, we investigate whether the presence of causality in extreme volatility can be linked to some business cycle and/or financial conditions.

For much of the 20th century, global finance was more patchwork than network. But the past thirty years have seen that picture change spectacularly and global finance is now a well-connected network. Within some limits, such connectivity acts as a shock-absorber and links in the system behave as a mutual insurance device that help distribute and disperse risk. But when shocks are sufficiently large, connectivity may instead serve as a shock-transmitter. Risk-sharing becomes risk spreading and links in the system play the role of a mutual incendiary device that amplifies risk. Understanding the robustness and

magnitude of links between business cycle state variables and extreme volatility transmission represents an important empirical question in finance since it is a consequential input for asset allocation decisions, risk management and macroprudential policies.

We start the empirical investigation by checking for the presence of extreme causality dynamically from the US equity market (by relying on the SP500 index) to six European equity markets (the FTSE, DAX, CAC, AEX, IBEX and MIB indices are representative for UK, Germany, France, Holland, Spain and Italy, respectively). The analysis is performed in a dynamic setup based on 696 rolling windows (defined by a weekly step), each one including 500 observations (which is the equivalent of two years of stock-market data). We set α to 95%, H to 10 lags and use the 5-minutes bi-power variation realized measure of variance. The causality test in extreme variance from US to Europe (proposed in Section 3) is implemented for each of the six European countries separately.

Figure 3 presents the test-statistic $\widehat{Q}(H)_{t-500:t}$ from 2002 to 2016 for each European country and the critical $\chi_{95\%}^2(H)$ value for a significance level $\eta = 5\%$, represented by a horizontal dashed line. Two important observations can be made. First, extreme volatility contagion is not constant but time-varying: periods of extreme variance transmission and periods when there is no transmission alternate. It is clear for the naked eye that, for example, during the global financial crisis the extreme volatility in US was transmitted to all European countries. Second, extreme volatility contagion from the US equity market is not homogeneous across European Equity Markets suggesting an imperfect financial integration in Europe and Eurozone more specifically. For example, Italy and Spain seems more subject to US spillovers than Germany or UK. Also, some countries appear to be more affected by US contagion over the periods 2003-2004 and 2015-2016.

Next, we investigate whether extreme volatility transmission could be linked to macroeconomic development. While the behavior of aggregate volatility and its business cycle dependence are well documented (e.g. Schwert, 1989; Diebold and Yilmaz, 2012; Paye, 2012), empirical analyses of volatility transmission factors are less common. Based on the previous observation that contagion peaked for some countries during 2003-2004, 2008-2009 and 2015-2016, we choose to focus on the US monetary business cycles and gauge their correlation with extreme volatility transmission between US and European financial markets. Indeed these periods were marked by intense changes in the stance of the US monetary policy.

Historically, the Federal Reserve (hereafter, the Fed) has used the federal funds rate as the primary instrument of monetary policy, lowering the rate to provide more stimulus and raising it to slow economic activity and control inflation. But between December 2008 and December 2015, the federal funds rate has been near zero, so that lowering it further to

produce more stimulus has not been an option. Consequently, the Fed has relied on unconventional policy tools such as large-scale asset purchases (commonly known as quantitative easing or QE) and forward guidance to amend long-term interest rates and influence the economy. In this “zero lower bound” environment, a number of researchers used shadow rate models to quantify the stance of monetary policy (e.g. Krippner, 2013). We therefore use the shadow rates to proxy the US monetary business stance. When the estimated shadow fed funds rate is at least 25 basis points, the effective federal funds rate is used. Figure 4 presents the US shadow (fed fund) rate and the 2-year rolling range of this rate. This Figure illustrates the US monetary cycles over the period with successive waves of easing (2000-2003 and 2007-2013) and tightening (2004-2006 and 2013-2016).

In a regression model we relate the level of inter-market dependence to the shadow rates while conditioning upon the presence (absence) of causality. Along the lines of Christiansen et al. (2012), we also include, as control variables, the TED spread (hereafter TEDS) calculated as the spread between 3-month LIBOR based on USD and 3-month Treasury Bill. The data spans the period from January 4, 2000 to September 23, 2016 and it has been collected from three sources: i) the realized measures of variance are taken from the realized library” at Oxford-Man Institute, ii) the control variable and the effective federal funds rate are found in the Federal Reserve Economic database, and iii) the shadow rates come from Krippner (2013) updates.

To check if the presence of causality in variance is related to the dynamics of the shadow rates variable, we estimate the following regression

$$\log \widehat{Q}(H) = \beta_0 + \beta_1 SRI_{\widehat{Q}(H) > \chi_{0.95}^2(H)} + \beta_2 SR + \delta_1 TEDS + \varepsilon,$$

where $\widehat{Q}(H)$ is the vector of causality in extreme variance test-statistics, and SR is the associated vector of ranges of the US shadow rate. SR is computed over the same rolling windows (of 500 observations) where we applied our causality test so as to capture the variability, and to some extent the instability, of the monetary policy over each subsample where we applied our causality test.

Table 11 presents the estimation results for the US shadow rate along with the associated HAC t-statistics for each country pair. Given the strong persistence of the variables, the HAC t-statistics are computed by following Sun (2004) with a bandwidth of 0.1. The results of interest in Table 11 are the slope parameters β_1 associated with the causality regime. They are generally positive and significant, indicating that the dynamics of the shadow rates is strongly related with the presence of causality from US to European equity markets. In particular, more variability in the shadow rates is accompanied by an increase in the log of the test-statistic, i.e., a stronger rejection of the non-causality. This can be due

either to changes in the monetary policy as a reaction to the business cycle development and/or to monetary policy decisions that subsequently affect the financial markets such as the “taper tantrum” episode in 2013 suggests. This result is even stronger, as the tail interaction term actually captures all existing dependence between the presence of causality in variance and the dynamics of the shadow rates. The non-significance of β_2 indeed reflects the absence of relationship in the center of the distribution. Besides, except for Germany, the control variable does not appear to be significant, which indicates that funding risks on the US market are not related to the presence of causality in extreme variance toward the European markets. In a nutshell, extreme volatility transmission seems to be intimately related to the dynamics of the US shadow rate and hence the US monetary policy.

7 Conclusion

We proposed a Granger-causality test in extreme variance. As the variance is unobserved, our testing strategy is based on realized measures of the integrated variance. In particular, the test relies on the cross-lagged correlation between tail-event indicator functions derived from a quantile HAR model for realized measures of variance associated with each of the two financial series considered. The feasible testing procedure is semiparametric and asymptotically free of estimation risk that may arise from the approximation of the integrated variance by realized measures, or from the estimation of its conditional quantiles in the HARQ specification. The resulting Ljung-Box type test-statistic has a traditional chi-square asymptotic distribution and it is simple to implement. Extensive Monte-Carlo simulations show that our test has good finite-sample properties. In particular, it exhibits high power for both the IV and QV realized measures regardless of way causality is specified under the alternative hypothesis, i.e. causality in the continuous and / or the discontinuous jump component of the quadratic variation. A natural extension of our Granger causality test in extreme variance focuses on the whole quadratic variation by using, for instance, the realized variance estimator.

Finally, we propose an empirical illustration that looks into extreme volatility transmission from the US equity market to six European ones from 2002 to 2016. Without loss of generality, the bi-power variation realized measure is used. Our test identifies periods where causality in extreme variance is significant and relates the intensity of the volatility transmission to the US monetary business cycle, in particular through the shadow rates. The US monetary policy hence contributes to set the tone not only for credit conditions worldwide in terms of volumes and prices but also for extreme volatility transmission across the world.

References

- Y. Aït-Sahalia and L. Mancini. Out of sample forecasts of quadratic variation. *Journal of Econometrics*, 147(1):17–33, 2008.
- T. Andersen and L. Benzoni. Realized volatility. *edited by Andersen, T G, Richard A Davis, J P Kreiss and Thomas Mikosch in "Handbook of Financial Time Series*, Springer-Verlag: 555–575, 2009.
- T. G. Andersen, T. Bollerslev, F. X. Diebold, and P. Labys. Modeling and forecasting realized volatility. *Econometrica*, 71:529–626, 2003.
- T. G. Andersen, D. Dobrev, and E. Schaumburg. Jump-robust volatility estimation using nearest neighbor truncation. *Journal of Econometrics*, 169(1):75–93, 2012.
- L. Baele. Volatility spillover effects in european equity markets. *Journal of Financial and Quantitative Analysis*, 40(02):373–401, 2005.
- O. Barndorff-Nielsen, P. R. Hansen, A. Lunde, and N. Shephard. Designing realized kernels to measure the ex post variation of equity prices in the presence of noise. *Econometrica*, 76(6):1481–1536, 2008.
- O. E. Barndorff-Nielsen and N. Shephard. Power and bipower variation with stochastic volatility and jumps (with discussion). *Journal of Financial Econometrics*, 2:1–37, 2004.
- M. Bibinger and L. Winkelmann. Econometrics of co-jumps in high-frequency data with noise. *Journal of Econometrics*, 184(2):361–378, 2015.
- T. Bollerslev, J. Litvinova, and G. Tauchen. Leverage and volatility feedback effect in high-frequency data. *Journal of Financial Econometrics*, 4(3):353–384, 2006.
- L. Cappiello, B. Gérard, A. Kadareja, and S. Manganelli. Measuring comovements by regression quantiles. *Journal of Financial Econometrics*, 12(4):645–678, 2014.
- W. H. Chan and J. M. Maheu. Conditional jump dynamics in stock market returns. *Journal of Business and Economic Statistics*, 79:377–389, 2002.
- Y. W. Cheung and L. K. Ng. A causality-in-variance test and its application to financial market prices. *Journal of Econometrics*, 72:33–48, 1996.
- K. Christensen, R. Oomen, and M. Podolskij. Realised quantile-based estimation of the integrated variance. *Journal of Econometrics*, 159(1):74–98, 2010.

- C. Christiansen, M. Schmeling, and A. Schrimpf. A comprehensive look at financial volatility prediction by economic variables. *Journal of Applied Econometrics*, 27(6):956–977, 2012.
- P. F. Christoffersen. Evaluating interval forecasts. *International economic review*, pages 841–862, 1998.
- V. Corradi, W. Distaso, and M. Fernandes. International market links and volatility transmission. *Journal of Econometrics*, 170(1):117–141, 2012.
- F. Corsi. A simple approximate long-memory model of realized volatility. *Journal of Financial Econometrics*, 7:174–196, 2009.
- F. X. Diebold and K. Yilmaz. Better to give than to receive: Predictive directional measurement of volatility spillovers. *International Journal of Forecasting*, 28(1):57–66, 2012.
- R. F. Engle and V. Ng. Measuring and testing the impact of news on volatility. *Journal of Finance*, 48:1749–1778, 1988.
- R. F. Engle, T. Ito, and W.-L. Lin. Meteor showers or heat waves: Heteroskedastic intradaily volatility in the foreign exchange market. *Econometrica*, 58:525–542, 1990.
- K. J. Forbes and R. Rigobon. No contagion, only interdependence: measuring stock market comovements. *The journal of Finance*, 57(5):2223–2261, 2002.
- J.-Y. Gnabo, L. Hvozdyk, and J. Lahaye. System-wide tail comovements: A bootstrap test for cojump identification on the s&p 500, us bonds and currencies. *Journal of International Money and Finance*, 48:147–174, 2014.
- C. W. J. Granger, R. P. Robins, and R. F. Engle. Wholesale and retail prices: Bivariate time series modelling with forecastable error variances. *in: D. Belsley and E. Kuh, eds., Model Reliability, MIT Press, Cambridge, MA*, pages 1–17, 1986.
- C. M. Hafner and H. Herwartz. Testing for causality in variance using multivariate garch models. *Annals of Economics and Statistics*, 89:215–241, 2008.
- H. Han, O. Linton, T. Oka, and Y.-J. Whang. The cross-quantilogram: Measuring quantile dependence and testing directional predictability between time series. *Journal of Econometrics*, 193(1):251–270, 2016.
- E. J. Hannan. The asymptotic distribution of serial covariances. *The Annals of Statistics*, pages 396–399, 1976.

- P. R. Hansen and A. Lunde. Realized variance and market microstructure noise. *Journal of Business and Economic Statistics*, 24(2):127–161, 2006.
- Y. Hong. A test for volatility spillover with application to exchange rates. *Journal of Econometrics*, 103:183–224, 2001.
- Y. Hong, Y. Liu, and W. S. Granger causality in risk and detection of extreme risk spillover between financial markets. *Journal of Econometrics*, 150:271–287, 2009.
- J. Jacod and V. Todorov. Testing for common arrivals of jumps for discretely observed multidimensional processes. *The Annals of Statistics*, pages 1792–1838, 2009.
- K. Jeong, W. K. Härdle, and S. Song. A consistent nonparametric test for causality in quantile. *Econometric Theory*, 28(04):861–887, 2012.
- R. Koenker and G. Bassett Jr. Regression quantiles. *Econometrica: journal of the Econometric Society*, pages 33–50, 1978.
- L. Krippner. Measuring the stance of monetary policy in zero lower bound environments. *Economics Letters*, 118(1):135–138, 2013.
- G. M. Ljung and G. E. Box. On a measure of lack of fit in time series models. *Biometrika*, 65(2):297–303, 1978.
- M. McAleer and M. C. Medeiros. A multiple regime smooth transition heterogeneous autoregressive model for long memory and asymmetries. *Journal of Econometrics*, 147(1):104–119, 2008a.
- M. McAleer and M. C. Medeiros. Realized volatility: a review. *Econometric Reviews*, 27:10–45, 2008b.
- N. Meddahi. Arma representation of integrated and realized variances. *Econometrics Journal*, 6:335–356, 2003.
- B. S. Paye. déjà vol: Predictive regressions for aggregate stock market volatility using macroeconomic variables. *Journal of Financial Economics*, 106(3):527–546, 2012.
- R. Roy. Asymptotic covariance structure of serial correlations in multivariate time series. *Biometrika*, 76(4):824–827, 1989.
- G. W. Schwert. Margin requirements and stock volatility. *Journal of Financial Services Research*, 3(2-3):153–164, 1989.

- M. Sensier and D. van Dijk. Testing for volatility changes in u.s. macroeconomic time series. *Review of Economics and Statistics*, 86:833–839, 2004.
- M. Soucek and N. Todorova. Realized volatility transmission: The role of jumps and leverage effects. *Economics Letters*, 122(2):111–115, 2014.
- Y. Sun. A convergent t-statistic in spurious regressions. *Econometric Theory*, 20(05):943–962, 2004.
- V. Todorov and G. Tauchen. Volatility jumps. *Journal of Business and Economic Statistics*, 29(3):356–371, 2011.
- F. Zikes and J. Barunik. Semi-parametric conditional quantile models for financial returns and realized volatility. *Journal of Financial Econometrics*, 0(0):1–42, 2014.

Acknowledgments

We thank Torben Andersen, Peter Hansen, Christophe Hurlin, Sebastien Laurent, Rachidi Kotchoni, Arthur Charpentier, the participants at the 2016 EC² conference on *Big Data* and the 8th French Econometrics Conference, and the seminar participants at Orléans and Paris-Nanterre, for helpful comments and suggestions.

A Appendix A: Proof of Lemmas

A.1 Proof of Lemma 1

Lemma 1: Under the null hypothesis of absence of causality in extreme variance, as $T \rightarrow \infty$

$$Q^*(H) \sim \chi_H^2, \quad (30)$$

where χ_H^2 is the chi-square random variable with H degrees of freedom.

Proof: The infeasible test statistic $Q^*(H)$ is defined as

$$Q^*(H) = T(T+2) \sum_{h=1}^H \frac{\rho^{*2}(h)}{T-h}, \quad (31)$$

with $\rho^*(h)$ the cross-lagged correlation of order h between $z_{1,t}(\alpha)$ and $z_{2,t}(\alpha)$. Note that $\{z_{1,t}(\alpha)\}$ is independent of $\{z_{2,s}(\alpha), s < t\}$. Moreover, both $z_{1,t}(\alpha)$ and $z_{2,t}(\alpha)$ are i.i.d. sequences, because they are defined as quantile-exception processes. This can be regarded

by analogy with the risk-management literature where the IIDness property of a quantile-exception process is used to backtest quantile or value-at-risk models (Christoffersen, 1998). Hence, it follows from Hannan (1976) and Roy (1989) that as $T \rightarrow \infty$

$$\sqrt{T}(\rho^*(1), \rho^*(2), \dots, \rho^*(H))' \sim N(0, I_H), \quad (32)$$

with I_H the identity matrix of dimension H , and therefore

$$\frac{T(T+2)}{T-h} \rho^{*2}(h) \sim \chi^2(1), \quad \forall h = 1, \dots, H, \quad (33)$$

which completes the proof. \square

A.2 Proof of Lemma 2

Lemma 2: Under Assumptions 2 and 3, as $T \rightarrow \infty$

$$\widehat{Q}(H) - Q(H) = o_p(1). \quad (34)$$

Proof: Recall that $\widehat{Q}(H)$ is the feasible test statistic based on the cross-lagged correlation between the estimated event variables $z_{1,t,M}(\alpha; \widehat{\theta}_1)$ and $z_{2,t,M}(\alpha; \widehat{\theta}_2)$, while $Q(H)$ is the infeasible counterpart based on the cross-lagged correlation between $z_{1,t,M}(\alpha; \theta_1^0)$ and $z_{2,t,M}(\alpha; \theta_2^0)$. We denote $\rho(h)$ the cross-lagged correlation of order h , $h = 1, \dots, H$, between $z_{1,t,M}(\alpha; \theta_1^0)$ and $z_{2,t,M}(\alpha; \theta_2^0)$, which is the unfeasible counterpart of $\widehat{\rho}(h)$ as defined in (8). $\widehat{C}(h)$ is the cross-lagged covariance associated with $\widehat{\rho}(h)$, and $C(h)$ its unfeasible counterpart associated with $\rho(h)$. Consequently, we have that

$$\widehat{Q}(H) - Q(H) = \frac{1}{\pi^2(1-\pi)^2} \sum_{h=1}^H \frac{T(T+2)}{(T-h)} \left(\widehat{C}(h)^2 - C(h)^2 \right). \quad (35)$$

The rest of the proof proceeds by showing that $\widehat{C}(h)^2 - C(h)^2 = o_p(1)$. Note that

$$\widehat{C}(h)^2 - C(h)^2 = A + B, \quad (36)$$

with

$$A = \left(\widehat{C}(h) - C(h) \right)^2, \quad (37)$$

$$B = 2 \left(\widehat{C}(h) - C(h) \right) C(h). \quad (38)$$

Using the definition of both $\widehat{C}(h)$ and $C(h)$, the difference $\widehat{C}(h) - C(h)$ can be written as

$$\widehat{C}(h) - C(h) = T^{-1} \sum_{t=1}^T \left\{ \widehat{I}_t \left(\widehat{\theta}_1, \widehat{\theta}_2 \right) - I_t \left(\theta_1^0, \theta_2^0 \right) \right\}, \quad (39)$$

with

$$\widehat{I}_t \left(\widehat{\theta}_1, \widehat{\theta}_2 \right) = z_{1,t,M} \left(\alpha; \widehat{\theta}_1 \right) z_{2,t-h,M} \left(\alpha; \widehat{\theta}_2 \right), \quad (40)$$

$$I_t(\theta_1^0, \theta_2^0) = z_{1,t,M}(\alpha; \theta_1^0) z_{2,t-h,M}(\alpha; \theta_2^0). \quad (41)$$

For the rest of the proof we build on Cappiello et al. (2014, Proof of Theorem 1). Let $u_{i,t} = IV_{i,t,M} - q_{i,t,M}(\alpha, \theta_i^0)$ be the true quantile residuals, and $\delta_{i,t}(\widehat{\theta}_i) = q_{i,t,M}(\alpha, \widehat{\theta}_i) - q_{i,t,M}(\alpha, \theta_i^0)$. Since $z_{i,t,M}(\alpha, \widehat{\theta}_i) = \mathbb{I}(IV_{i,t,M} \geq q_{i,t,M}(\alpha, \widehat{\theta}_i))$, we have $z_{i,t,M}(\alpha, \widehat{\theta}_i) = \mathbb{I}(u_{i,t} \geq \delta_{i,t}(\widehat{\theta}_i))$ and $z_{i,t,M}(\alpha, \theta_i^0) = \mathbb{I}(u_{i,t} \geq 0)$. It follows that

$$\begin{aligned} \left| I_t(\widehat{\theta}_1, \widehat{\theta}_2) - I_t(\theta_1^0, \theta_2^0) \right| &= \left| z_{1,t,M}(\alpha, \widehat{\theta}_1) z_{2,t-h,M}(\alpha, \widehat{\theta}_2) - z_{1,t,M}(\alpha, \theta_1^0) z_{2,t-h,M}(\alpha, \theta_2^0) \right| \quad (42) \\ &= \left| \mathbb{I}(u_{1,t} \geq \delta_{1,t}(\widehat{\theta}_1)) \mathbb{I}(u_{2,t-h} \geq \delta_{2,t-h}(\widehat{\theta}_2)) - \mathbb{I}(u_{1,t} \geq 0) \mathbb{I}(u_{2,t-h} \geq 0) \right|. \end{aligned}$$

Now suppose that $\delta_{i,t}(\widehat{\theta}_i) < 0, \forall t$ (the same reasoning applies for $\delta_{i,t}(\widehat{\theta}_i) > 0$). Using the fact that $ab - cd = (a - c)d + c(b - d) + (a - c)(b - d)$, we obtain (42)

$$\begin{aligned} \left| I_t(\widehat{\theta}_1, \widehat{\theta}_2) - I_t(\theta_1^0, \theta_2^0) \right| &= \left| \left(\mathbb{I}(u_{1,t} \geq \delta_{1,t}(\widehat{\theta}_1)) - \mathbb{I}(u_{1,t} \geq 0) \right) \mathbb{I}(u_{2,t-h} \geq 0) + \right. \\ &\quad \left. + \mathbb{I}(u_{1,t} \geq 0) \left(\mathbb{I}(u_{2,t-h} \geq \delta_{2,t-h}(\widehat{\theta}_2)) - \mathbb{I}(u_{2,t-h} \geq 0) \right) + \right. \\ &\quad \left. + \left(\mathbb{I}(u_{1,t} \geq \delta_{1,t}(\widehat{\theta}_1)) - \mathbb{I}(u_{1,t} \geq 0) \right) \times \right. \\ &\quad \left. \times \left(\mathbb{I}(u_{2,t-h} \geq \delta_{2,t-h}(\widehat{\theta}_2)) - \mathbb{I}(u_{2,t-h} \geq 0) \right) \right| \quad (43) \\ &= \mathbb{I}(\delta_{1,t}(\widehat{\theta}_1) \leq u_{1,t} \leq 0) \mathbb{I}(u_{2,t-h} \geq 0) + \\ &\quad + \mathbb{I}(u_{1,t} \geq 0) \mathbb{I}(\delta_{2,t-h}(\widehat{\theta}_2) \leq u_{2,t-h} \leq 0) + \\ &\quad + \mathbb{I}(\delta_{1,t}(\widehat{\theta}_1) \leq u_{1,t} \leq 0) \mathbb{I}(\delta_{2,t-h}(\widehat{\theta}_2) \leq u_{2,t-h} \leq 0) \\ &\leq 2\mathbb{I}(\delta_{1,t}(\widehat{\theta}_1) \leq u_{1,t} \leq 0) + \mathbb{I}(\delta_{2,t-h}(\widehat{\theta}_2) \leq u_{2,t-h} \leq 0). \quad (44) \end{aligned}$$

By applying the mean value theorem to the expectation of the first term in (44), we have

$$\begin{aligned} \mathbb{E} \left(\mathbb{I}(\delta_{1,t}(\widehat{\theta}_1) \leq u_{1,t} \leq 0) \right) &= \mathbb{E} \left(\left| \int_{\delta_{1,t}(\widehat{\theta}_1)}^0 g_{1,t}(u_1) du_1 \right| \right) \\ &= \mathbb{E} \left(\left| -g_{1,t}(\varepsilon) \nabla q_{1,t,M}(\alpha, \theta_1^*) (\widehat{\theta}_1 - \theta_1^0) \right| \right), \quad (45) \end{aligned}$$

where $g_{1,t}(\cdot)$ is the *p.d.f.* of the quantile residuals $IV_{1,t,M} - q_{1,t,M}(\alpha, \theta_1^0)$, $\delta_{1,t}(\widehat{\theta}_1) < \varepsilon < 0$, and θ_1^* lies between $\widehat{\theta}_1$ and θ_1^0 . Using Assumptions 2 and 3, Equation (45) then becomes

$$\begin{aligned} \mathbb{E} \left(\mathbb{I}(\delta_{1,t}(\widehat{\theta}_1) \leq u_{1,t} \leq 0) \right) &\leq \mathbb{E} |UdK(\mathcal{G}_{1,t})| \\ &\leq \mathbb{E} |UdK_0| = O(d) \end{aligned}$$

for d arbitrarily small and T large enough such that $\|\widehat{\theta}_1 - \theta_1^0\| \leq d$. Similar arguments can be used for the second term in (44) to show that $\mathbb{E} \left(\mathbb{I}(\delta_{2,t-h}(\widehat{\theta}_2) \leq u_{2,t-h} \leq 0) \right) = O(d)$. Hence, following Cappiello et al. (2014), since d can be chosen arbitrarily small, these results

imply that $T^{-1} \sum_{t=1}^T \{\widehat{I}_t(\widehat{\theta}_1, \widehat{\theta}_2) - I_t(\theta_1^0, \theta_2^0)\} = o_p(1)$, and $\widehat{C}(h) - C(h) = o_p(1)$. It can be easily deduced that $A = o_p(1)$, and $B = o_p(1)$ and therefore $\widehat{C}(h)^2 - C(h)^2 = o_p(1)$. This completes the proof. \square

A.3 Proof of Lemma 3

Lemma 3: Under Assumption 1, if $T^{\frac{1}{k-1}} b_M^{-1/2} \rightarrow 0$, as $T, M \rightarrow \infty$, we have

$$Q(H) - Q^*(H) = o_p(1). \quad (46)$$

Proof: The infeasible test statistic $Q^*(H)$ is based on the cross-lagged correlation (or covariance) between $z_{1,t}(\alpha)$ and $z_{2,t}(\alpha)$, the tail-event variables for the true processes of integrated variance. Using the same reasoning as in the proof of Lemma 7, we have

$$Q(H) - Q^*(H) = \frac{1}{\pi^2(1-\pi)^2} \sum_{h=1}^H \frac{T(T+2)}{(T-h)} (C(h)^2 - C^*(h)^2), \quad (47)$$

where again $C(h)$ is the cross-lagged covariance of order h between $z_{1,t,M}(\alpha; \theta_1^0)$ and $z_{2,t,M}(\alpha; \theta_2^0)$, the tail-event variables for the realized measure of integrated variance and $C^*(h)$ is the same statistic but involving $z_{1,t}(\alpha)$ and $z_{2,t}(\alpha)$. We then proceed by showing that $C(h)^2 - C^*(h)^2 = o_p(1)$. As above, we rewrite $C(h)^2 - C^*(h)^2$ as

$$C(h)^2 - C^*(h)^2 = A_1 + A_2, \quad (48)$$

with

$$A_1 = (C(h) - C^*(h))^2, \quad (49)$$

$$A_2 = 2(C(h) - C^*(h))C^*(h). \quad (50)$$

Now, let us study the asymptotic behavior of $C(h) - C^*(h)$. We have that

$$C(h) - C^*(h) = T^{-1} \sum_{t=1}^T \{I_t(\theta_1^0, \theta_2^0) - I_t^*(\theta_1^0, \theta_2^0)\}, \quad (51)$$

with

$$I_t(\theta_1^0, \theta_2^0) = z_{1,t,M}(\alpha; \theta_1^0) z_{2,t-h,M}(\alpha; \theta_2^0), \quad (52)$$

$$I_t^*(\theta_1^0, \theta_2^0) = z_{1,t}(\alpha; \theta_1^0) z_{2,t-h}(\alpha; \theta_2^0). \quad (53)$$

Equivalently,

$$C(h) - C^*(h) = B_1 + B_2, \quad (54)$$

with

$$B_1 = T^{-1} \sum_{t=1}^T (z_{1,t,M}(\alpha; \theta_1^0) - z_{1,t}(\alpha; \theta_1^0)) z_{2,t-h,M}(\alpha; \theta_2^0), \quad (55)$$

$$B_2 = T^{-1} \sum_{t=1}^T (z_{2,t-h,M}(\alpha; \theta_2^0) - z_{2,t-h}(\alpha; \theta_2^0)) z_{1,t}(\alpha; \theta_1^0). \quad (56)$$

By the triangular inequality and assumption 1 it follows that

$$|C(h) - C^*(h)| \leq |B_1| + |B_2|, \quad (57)$$

where

$$|B_1| = \left| T^{-1} \sum_{t=1}^T (\mathbb{I}(y_{1,t,M} \leq 0) - \mathbb{I}(y_{1,t} \leq 0)) \mathbb{I}(y_{2,t-h,M} \leq 0) \right|, \quad (58)$$

$$|B_2| = \left| T^{-1} \sum_{t=1}^T (\mathbb{I}(y_{2,t-h,M} \leq 0) - \mathbb{I}(y_{2,t-h} \leq 0)) \mathbb{I}(y_{1,t} \leq 0) \right|, \quad (59)$$

from the definition of exceedances, with $\mathbb{I}(\cdot)$ the indicator function, and

$$\begin{aligned} y_{1,t} &= \theta_{1,1}^0 + \theta_{1,2}^0 IV_{1,t-1} + \theta_{1,3}^0 V_{1,t-1:t-5} + \theta_{1,4}^0 V_{1,t-1:t-22} - IV_{1,t}, \\ y_{1,t,M} &= \theta_{1,1}^0 + \theta_{1,2}^0 IV_{1,t-1,M} + \theta_{1,3}^0 V_{1,t-1:t-5,M} + \theta_{1,4}^0 V_{1,t-1:t-22,M} - IV_{1,t,M}, \\ y_{2,t} &= \theta_{2,1}^0 + \theta_{2,2}^0 IV_{2,t-1,M} + \theta_{2,3}^0 V_{2,t-1:t-5,M} + \theta_{2,4}^0 V_{2,t-1:t-22,M} - IV_{2,t,M}, \\ y_{2,t-h} &= \theta_{2,1}^0 + \theta_{2,2}^0 IV_{2,t-h-1} + \theta_{2,3}^0 V_{2,t-h-1:t-h-5} + \theta_{2,4}^0 V_{2,t-h-1:t-h-22} - IV_{2,t-h}, \\ y_{2,t-h,M} &= \theta_{2,1}^0 + \theta_{2,2}^0 IV_{2,t-h-1,M} + \theta_{2,3}^0 V_{2,t-h-1:t-h-5,M} + \theta_{2,4}^0 V_{2,t-h-1:t-h-22,M} - IV_{2,t-h,M}. \end{aligned}$$

In the following we focus on the asymptotic behavior of $|B_1|$ and derive that of $|B_2|$ by analogy. From Zikes and Barunik (2014) and by Cauchy-Schwarz inequality,

$$|B_1| \leq T^{-1} \sum_{t=1}^T |\mathbb{I}(y_{1,t,M} \leq 0) - \mathbb{I}(y_{1,t} \leq 0)| |\mathbb{I}(y_{2,t-h,M} \leq 0)|. \quad (60)$$

Using the expression of $y_{1,t,M}$ in terms of estimation error,

$$\begin{aligned} y_{1,t,M} &= y_{1,t} - (IV_{1,t,M} - IV_{1,t}) + \theta_{1,2}^0 (IV_{1,t-1,M} - IV_{1,t-1}) + \\ &\quad + \theta_{1,3}^0 (V_{1,t-1:t-5,M} - V_{1,t-1:t-5}) + \theta_{1,4}^0 (V_{1,t-1:t-22,M} - V_{1,t-1:t-22}) \\ &= y_{1,t} - N_{1,t,M} + \theta_{1,2}^0 N_{1,t-1,M} + \frac{\theta_{1,3}^0}{5} \sum_{j=1}^5 N_{1,t-j,M} + \frac{\theta_{1,4}^0}{22} \sum_{j=1}^{22} N_{1,t-j,M}, \end{aligned}$$

we obtain

$$\begin{aligned} |B_1| &\leq T^{-1} \sum_{t=1}^T \left| \mathbb{I} \left(y_{1,t} - N_{1,t,M} + \theta_{1,2}^0 N_{1,t-1,M} + \frac{\theta_{1,3}^0}{5} \sum_{j=1}^5 N_{1,t-j,M} + \frac{\theta_{1,4}^0}{22} \sum_{j=1}^{22} N_{1,t-j,M} \leq 0 \right) \right. \\ &\quad \left. - \mathbb{I}(y_{1,t} \leq 0) \right| |\mathbb{I}(y_{2,t-h,M} \leq 0)|, \end{aligned}$$

or equivalently,

$$|B_1| \leq T^{-1} \sum_{t=1}^T \mathbb{I}(-l \leq y_{1,t} \leq l) |\mathbb{I}(y_{2,t-h,M} \leq 0)|. \quad (61)$$

The upper bound l is equal to

$$l = \sup_t |N_{1,t,M}| + \bar{\theta}_{1,2} \sup_t |N_{1,t-1,M}| + \frac{\bar{\theta}_{1,3}}{5} \sum_{j=1}^5 \sup_t |N_{1,t-j,M}| + \frac{\bar{\theta}_{1,4}}{22} \sum_{j=1}^{22} \sup_t |N_{1,t-j,M}|, \quad (62)$$

where $\bar{\theta}_{1,2} = \sup \theta_{1,2}^0$, $\bar{\theta}_{1,3} = \sup \theta_{1,3}^0$, and $\bar{\theta}_{1,4} = \sup \theta_{1,4}^0$, and they are well defined in a compact set Θ_1 . Given Assumption 1, we further have that $\forall j \geq 0$, as $T, M \rightarrow \infty$

$$\begin{aligned} \Pr \left(\sup_t T^{-\frac{1}{k-1}} b_M^{1/2} |N_{1,t-j,M}| > \varepsilon \right) &\leq \sum_{t=1}^T \Pr \left(T^{-\frac{1}{k-1}} b_M^{1/2} |N_{1,t-j,M}| > \varepsilon \right) \\ &\leq \varepsilon^{-k} T^{1-\frac{k}{k-1}} b_M^{k/2} \mathbb{E} |N_{1,t-j,M}|^k \\ &\leq \varepsilon^{-k} T^{-\frac{1}{k-1}} b_M^{k/2} O \left(b_M^{-k/2} \right) \\ &\equiv o(1), \end{aligned}$$

where the second inequality arises from the Markov inequality. Consequently,

$$\sup_t |N_{1,t-j,M}| = O_p \left(T^{\frac{1}{k-1}} b_M^{-1/2} \right), \quad \forall j \geq 0. \quad (63)$$

Based on Equations (61, 62, 63), we can state that there exists a positive constant c such that

$$\begin{aligned} |B_1| &\leq T^{-1} \sum_{t=1}^T \mathbb{I} \left(-c\delta T^{\frac{1}{k-1}} b_M^{-1/2} \leq y_{1,t} \leq c\delta T^{\frac{1}{k-1}} b_M^{-1/2} \right) |\mathbb{I}(y_{2,t-h,M} \leq 0)| \\ &\equiv B'_1, \end{aligned} \quad (64)$$

with

$$\delta = 1 + \bar{\theta}_{1,2} + \frac{\bar{\theta}_{1,3}}{5} + \frac{\bar{\theta}_{1,4}}{22}. \quad (65)$$

By conditioning on a set on which (64) holds, we use Markov and Hölder inequalities to write

$$\begin{aligned} \Pr \left(B'_1 > a \right) &\leq \frac{1}{a} T^{-1} \sum_{t=1}^T \Pr \left(-c\delta T^{\frac{1}{k-1}} b_M^{-1/2} \leq y_{1,t} \leq c\delta T^{\frac{1}{k-1}} b_M^{-1/2} \right)^{1/2} \times \\ &\quad \times \mathbb{E} \left(\mathbb{I}(y_{2,t-h,M} \leq 0)^2 \right)^{1/2} \\ &\equiv o(1) \end{aligned}$$

for a positive constant a . This holds since

$$\Pr \left(-c\delta T^{\frac{1}{k-1}} b_M^{-1/2} \leq y_{1,t} \leq c\delta T^{\frac{1}{k-1}} b_M^{-1/2} \right) \rightarrow 0 \quad (66)$$

as $T^{\frac{1}{k-1}} b_M^{-1/2} \rightarrow 0$ when $T, M \rightarrow \infty$ and because

$$\mathbb{E} \left(\mathbb{I}(y_{2,t-h,M} \leq 0)^2 \right)^{1/2} = (\alpha(1-\alpha) + \alpha^2)^{1/2} = \alpha^{1/2} < \infty. \quad (67)$$

Note that $\mathbb{I}(y_{2,t-h,M} \leq 0)$ is Benouilli distributed with parameter α regardless of the fact that the IV is estimated. This follows from the definition of the true conditional quantile, that insures $\alpha\%$ of IID exceedances in all cases.

It follows that $|B_1| = o_p(1)$, and the same reasoning leads to $|B_2| = o_p(1)$. Consequently, $\sup_{\theta \in \Theta} |C(h) - C^*(h)| = o_p(1)$ and hence it can be easily deduced that $C(h)^2 - C^*(h)^2 = o_p(1)$. This completes the proof. \square

B Appendix B: Tables and Figures

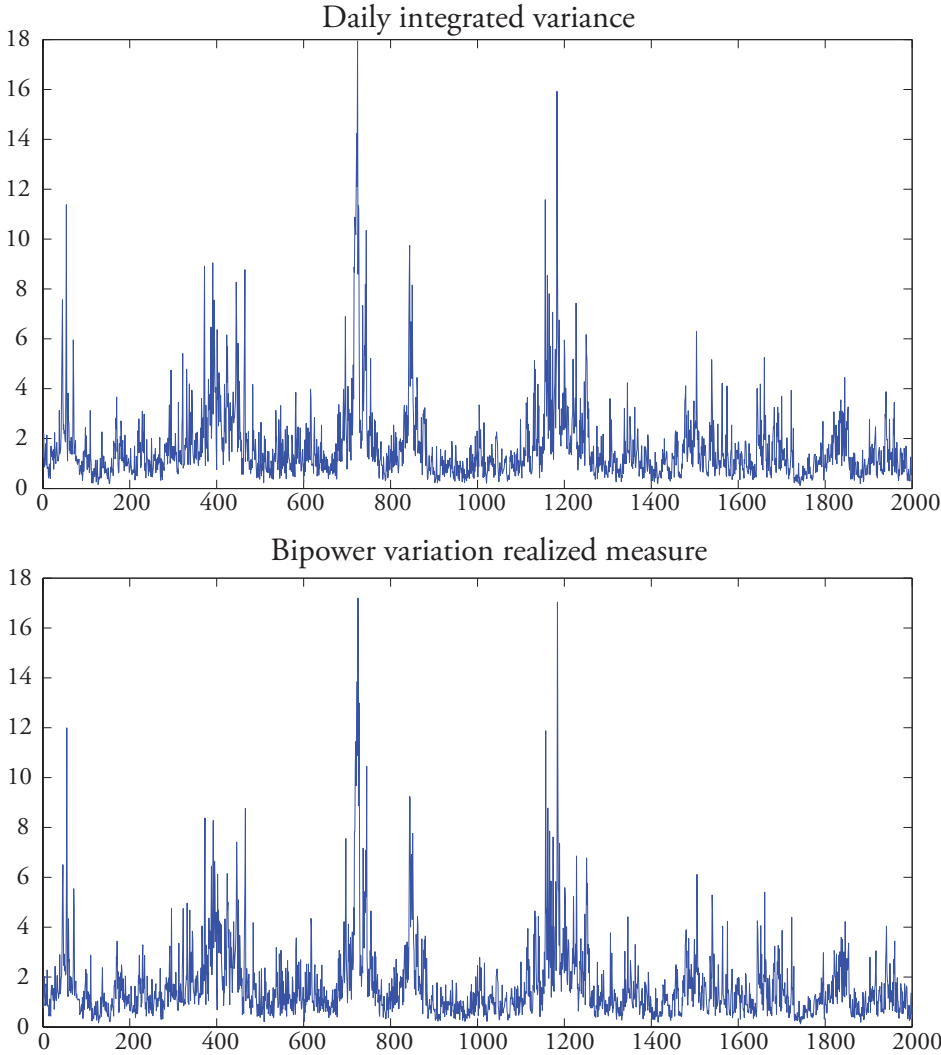


Figure 1: Simulated daily IV and BV realized measure with $M = 390$

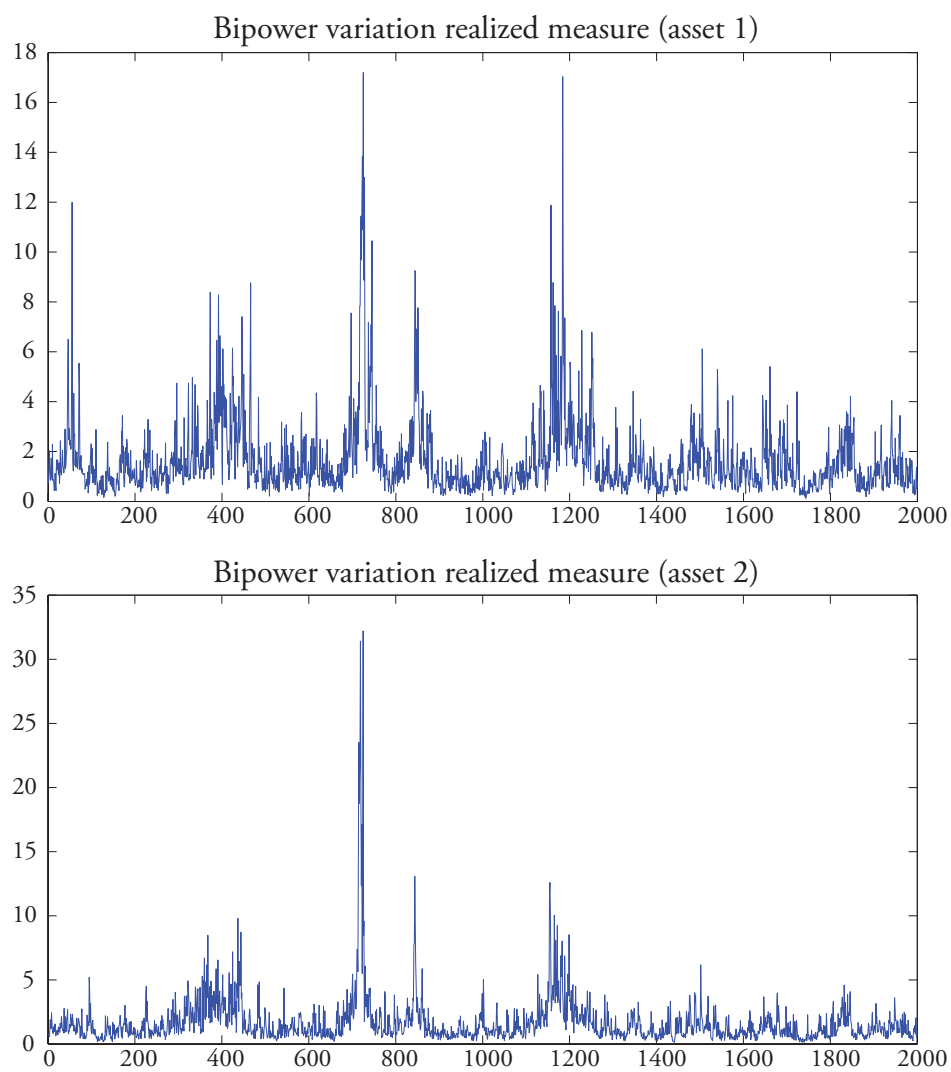


Figure 2: BV realized measures of the two assets with $M = 390$ and $\gamma = 0.5$

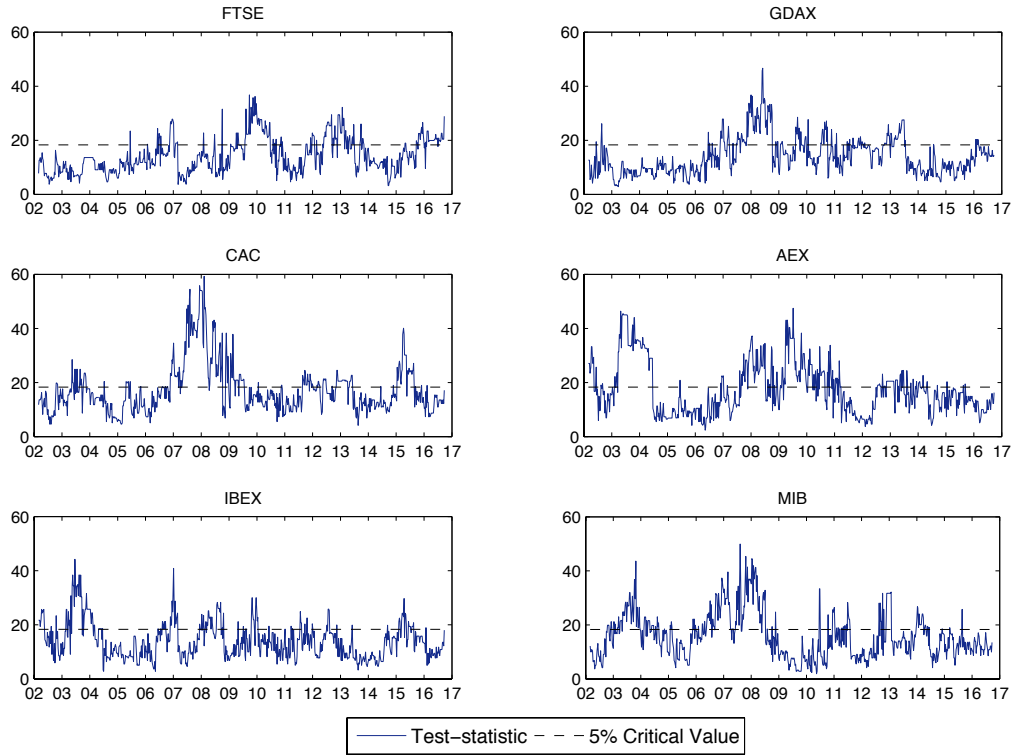


Figure 3: Causality in variance test

Note: This figure presents the test-statistic (computed on two-year rolling windows $s = 500$), $\widehat{Q}(H)_{t-s:t}$, for t going from 2002 to 2016.

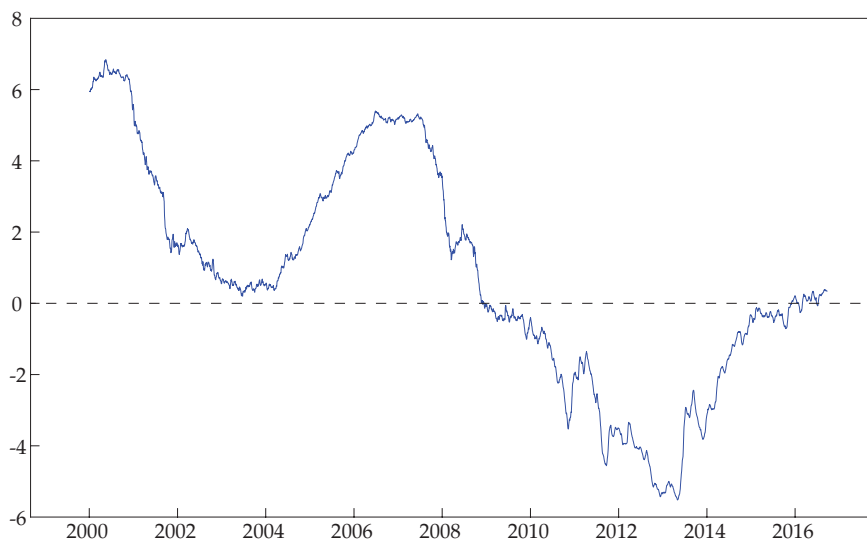


Figure 4: Shadow Rate Dynamics (Krippner 2013 updates)

Table 1: Empirical size of the causality test in extreme variance for the BPV measure

$\alpha = 90\%$				
	$M = 390$	$M = 78$	$M = 26$	$M = 13$
			H = 3	
$T = 500$	0.060	0.048	0.042	0.036
$T = 1000$	0.050	0.045	0.047	0.048
$T = 2000$	0.053	0.050	0.054	0.052
			H = 5	
$T = 500$	0.054	0.041	0.036	0.040
$T = 1000$	0.051	0.049	0.061	0.050
$T = 2000$	0.054	0.061	0.055	0.049
			H = 10	
$T = 500$	0.052	0.032	0.050	0.039
$T = 1000$	0.039	0.038	0.050	0.046
$T = 2000$	0.049	0.057	0.056	0.043
$\alpha = 95\%$				
	$M = 390$	$M = 78$	$M = 26$	$M = 13$
			H = 3	
$T = 500$	0.048	0.063	0.059	0.058
$T = 1000$	0.046	0.059	0.059	0.042
$T = 2000$	0.052	0.062	0.049	0.036
			H = 5	
$T = 500$	0.046	0.061	0.042	0.055
$T = 1000$	0.054	0.070	0.070	0.055
$T = 2000$	0.063	0.064	0.067	0.045
			H = 10	
$T = 500$	0.060	0.080	0.063	0.072
$T = 1000$	0.059	0.064	0.072	0.059
$T = 2000$	0.051	0.067	0.046	0.042

Notes: For a given value of the quadruplet (α, H, T, M) the Table displays the empirical size of the Granger-causality test in extreme variance, with α the confidence level, T the sample size (in days), M the number of intraday returns used to compute the realized measure of integrated variance, and H the maximum lag-order for the causality test. The nominal significance level η is set to 5%. The rejection frequencies are computed over 1000 simulations. The size results for the $medRV$ measure are strictly identical to those reported above.

Table 2: Empirical power of the causality test in extreme variance for the BPV measure with $\gamma = 0.5$

$\alpha = 90\%$				
	$M = 390$	$M = 78$	$M = 26$	$M = 13$
H = 3				
$T = 500$	0.255	0.267	0.275	0.257
$T = 1000$	0.489	0.471	0.464	0.413
$T = 2000$	0.784	0.780	0.736	0.697
H = 5				
$T = 500$	0.432	0.456	0.415	0.348
$T = 1000$	0.775	0.747	0.719	0.619
$T = 2000$	0.968	0.953	0.944	0.902
H = 10				
$T = 500$	0.362	0.375	0.335	0.310
$T = 1000$	0.681	0.679	0.639	0.562
$T = 2000$	0.946	0.935	0.919	0.872
$\alpha = 95\%$				
	$M = 390$	$M = 78$	$M = 26$	$M = 13$
H = 3				
$T = 500$	0.254	0.236	0.237	0.235
$T = 1000$	0.356	0.352	0.344	0.321
$T = 2000$	0.556	0.511	0.509	0.487
H = 5				
$T = 500$	0.382	0.367	0.337	0.318
$T = 1000$	0.562	0.559	0.539	0.507
$T = 2000$	0.815	0.785	0.758	0.706
H = 10				
$T = 500$	0.368	0.355	0.327	0.335
$T = 1000$	0.485	0.492	0.483	0.481
$T = 2000$	0.754	0.724	0.713	0.687

Notes: For a given value of the quadruplet (α, H, T, M) the Table displays the empirical power of the Granger-causality test in extreme variance, with α the confidence level, T the sample size (in days), M the number of intraday returns used to compute the realized measure of integrated variance, and H the maximum lag-order for the causality test. The nominal significance level η is set to 5%. The rejection frequencies are computed over 1000 simulations.

Table 3: Empirical power of the causality test in extreme variance for the $medRV$ measure with $\gamma = 0.5$

$\alpha = 90\%$				
	$M = 390$	$M = 78$	$M = 26$	$M = 13$
H = 3				
$T = 500$	0.276	0.253	0.265	0.248
$T = 1000$	0.491	0.462	0.470	0.432
$T = 2000$	0.780	0.757	0.738	0.708
H = 5				
$T = 500$	0.444	0.403	0.378	0.332
$T = 1000$	0.761	0.737	0.726	0.628
$T = 2000$	0.962	0.963	0.947	0.908
H = 10				
$T = 500$	0.377	0.352	0.330	0.297
$T = 1000$	0.691	0.674	0.649	0.570
$T = 2000$	0.936	0.936	0.931	0.891
$\alpha = 95\%$				
	$M = 390$	$M = 78$	$M = 26$	$M = 13$
H = 3				
$T = 500$	0.253	0.247	0.225	0.239
$T = 1000$	0.404	0.362	0.342	0.315
$T = 2000$	0.565	0.501	0.511	0.491
H = 5				
$T = 500$	0.368	0.364	0.357	0.329
$T = 1000$	0.586	0.567	0.542	0.482
$T = 2000$	0.810	0.767	0.752	0.710
H = 10				
$T = 500$	0.366	0.369	0.335	0.342
$T = 1000$	0.497	0.474	0.490	0.471
$T = 2000$	0.756	0.721	0.712	0.700

Notes: For a given value of the quadruplet (α, H, T, M) the Table displays the empirical power of the Granger-causality test in extreme variance, with α the confidence level, T the sample size (in days), M the number of intraday returns used to compute the realized measure of integrated variance, and H the maximum lag-order for the causality test. The nominal significance level η is set to 5%. The rejection frequencies are computed over 1000 simulations.

Table 4: Empirical power of the causality test in extreme variance for the BPV measure with $\gamma = 0.8$

$\alpha = 90\%$				
	$M = 390$	$M = 78$	$M = 26$	$M = 13$
H = 3				
$T = 500$	0.496	0.474	0.424	0.380
$T = 1000$	0.770	0.753	0.732	0.670
$T = 2000$	0.957	0.947	0.944	0.917
H = 5				
$T = 500$	0.694	0.668	0.610	0.532
$T = 1000$	0.935	0.929	0.896	0.859
$T = 2000$	0.989	0.990	0.989	0.980
H = 10				
$T = 500$	0.604	0.573	0.520	0.472
$T = 1000$	0.887	0.885	0.866	0.794
$T = 2000$	0.983	0.981	0.981	0.978
$\alpha = 95\%$				
	$M = 390$	$M = 78$	$M = 26$	$M = 13$
H = 3				
$T = 500$	0.356	0.366	0.337	0.328
$T = 1000$	0.555	0.539	0.534	0.499
$T = 2000$	0.779	0.767	0.722	0.682
H = 5				
$T = 500$	0.527	0.512	0.483	0.458
$T = 1000$	0.763	0.739	0.741	0.687
$T = 2000$	0.928	0.917	0.902	0.870
H = 10				
$T = 500$	0.478	0.477	0.469	0.425
$T = 1000$	0.675	0.661	0.655	0.602
$T = 2000$	0.877	0.880	0.845	0.842

Notes: For a given value of the quadruplet (α, H, T, M) the Table displays the empirical power of the Granger-causality test in extreme variance, with α the confidence level, T the sample size (in days), M the number of intraday returns used to compute the realized measure of integrated variance, and H the maximum lag-order for the causality test. The nominal significance level η is set to 5%. The rejection frequencies are computed over 1000 simulations.

Table 5: Empirical power of the causality test in extreme variance for the $medRV$ measure with $\gamma = 0.8$

$\alpha = 90\%$				
	$M = 390$	$M = 78$	$M = 26$	$M = 13$
H = 3				
$T = 500$	0.508	0.492	0.431	0.407
$T = 1000$	0.769	0.774	0.731	0.670
$T = 2000$	0.951	0.953	0.945	0.921
H = 5				
$T = 500$	0.724	0.686	0.612	0.552
$T = 1000$	0.948	0.936	0.900	0.864
$T = 2000$	0.987	0.987	0.992	0.980
H = 10				
$T = 500$	0.615	0.599	0.520	0.485
$T = 1000$	0.900	0.887	0.855	0.815
$T = 2000$	0.983	0.983	0.977	0.975
$\alpha = 95\%$				
	$M = 390$	$M = 78$	$M = 26$	$M = 13$
H = 3				
$T = 500$	0.366	0.375	0.358	0.310
$T = 1000$	0.541	0.543	0.543	0.486
$T = 2000$	0.785	0.775	0.730	0.698
H = 5				
$T = 500$	0.528	0.519	0.495	0.449
$T = 1000$	0.754	0.740	0.725	0.686
$T = 2000$	0.923	0.922	0.908	0.864
H = 10				
$T = 500$	0.476	0.473	0.463	0.444
$T = 1000$	0.655	0.685	0.646	0.630
$T = 2000$	0.887	0.868	0.868	0.838

Notes: For a given value of the quadruplet (α, H, T, M) the Table displays the empirical power of the Granger-causality test in extreme variance, with α the confidence level, T the sample size (in days), M the number of intraday returns used to compute the realized measure of integrated variance, and H the maximum lag-order for the causality test. The nominal significance level η is set to 5%. The rejection frequencies are computed over 1000 simulations.

Table 6: Empirical size of the causality test in extreme variance for the RK measure

$\alpha = 90\%$				
	$M = 390$	$M = 78$	$M = 26$	$M = 13$
H = 3				
T=500	0.044	0.039	0.044	0.043
T=1000	0.043	0.033	0.045	0.041
T=2000	0.042	0.046	0.052	0.047
H = 5				
T=500	0.042	0.044	0.043	0.052
T=1000	0.041	0.044	0.046	0.047
T=2000	0.054	0.053	0.052	0.063
H = 10				
T=500	0.038	0.043	0.036	0.058
T=1000	0.049	0.046	0.046	0.042
T=2000	0.058	0.036	0.062	0.047
$\alpha = 95\%$				
	$M = 390$	$M = 78$	$M = 26$	$M = 13$
H = 3				
T=500	0.060	0.070	0.068	0.060
T=1000	0.047	0.048	0.055	0.051
T=2000	0.052	0.050	0.045	0.045
H = 5				
T=500	0.046	0.047	0.047	0.054
T=1000	0.052	0.061	0.063	0.065
T=2000	0.059	0.063	0.055	0.036
H = 10				
T=500	0.068	0.065	0.054	0.058
T=1000	0.052	0.049	0.051	0.054
T=2000	0.050	0.055	0.056	0.052

Notes: For a given value of the quadruplet (α, H, T, M) the Table displays the empirical size of the Granger-causality test in extreme quadratic variation, with α the confidence level, T the sample size (in days), M the number of intraday returns used to compute the realized measure of quadratic variation, and H the maximum lag-order for the causality test. The nominal significance level η is set to 5%. The rejection frequencies are computed over 1000 simulations.

Table 7: Empirical power of the causality test in extreme variance for the RK measure

$\alpha = 90\%$				
	$M = 390$	$M = 78$	$M = 26$	$M = 13$
H = 3				
T=500	0.764	0.740	0.683	0.591
T=1000	0.978	0.974	0.940	0.909
T=2000	1.000	0.999	0.999	0.994
H = 5				
T=500	0.743	0.700	0.637	0.556
T=1000	0.975	0.962	0.935	0.890
T=2000	0.999	0.999	1.000	0.994
H = 10				
T=500	0.636	0.603	0.571	0.498
T=1000	0.948	0.929	0.909	0.828
T=2000	0.999	0.998	0.999	0.991
$\alpha = 95\%$				
	$M = 390$	$M = 78$	$M = 26$	$M = 13$
H = 3				
T=500	0.498	0.475	0.435	0.403
T=1000	0.768	0.716	0.690	0.618
T=2000	0.957	0.948	0.921	0.870
H = 5				
T=500	0.46	0.426	0.384	0.367
T=1000	0.741	0.688	0.654	0.600
T=2000	0.954	0.937	0.916	0.858
H = 10				
T=500	0.412	0.400	0.357	0.334
T=1000	0.652	0.600	0.581	0.508
T=2000	0.922	0.887	0.862	0.786

Notes: For a given value of the quadruplet (α, H, T, M) the Table displays the empirical power of the Granger-causality test in extreme quadratic variation, with α the confidence level, T the sample size (in days), M the number of intraday returns used to compute the realized measure of quadratic variation, and H the maximum lag-order for the causality test. Under the alternative hypothesis, we allow for causality in both the IV and the jump processes. The nominal significance level η is set to 5%. The rejection frequencies are computed over 1000 simulations.

Table 8: Empirical power of the causality test in extreme variance for the BV measure

$\alpha = 90\%$				
	$M = 390$	$M = 78$	$M = 26$	$M = 13$
H = 3				
T=500	0.296	0.279	0.285	0.293
T=1000	0.508	0.507	0.509	0.490
T=2000	0.786	0.811	0.806	0.768
H = 5				
T=500	0.491	0.431	0.368	0.351
T=1000	0.782	0.725	0.683	0.631
T=2000	0.963	0.952	0.947	0.909
H = 10				
T=500	0.410	0.349	0.332	0.304
T=1000	0.711	0.659	0.639	0.591
T=2000	0.945	0.934	0.929	0.893
$\alpha = 95\%$				
	$M = 390$	$M = 78$	$M = 26$	$M = 13$
H = 3				
T=500	0.263	0.265	0.278	0.251
T=1000	0.375	0.342	0.403	0.350
T=2000	0.532	0.530	0.558	0.526
H = 5				
T=500	0.382	0.381	0.342	0.302
T=1000	0.583	0.550	0.544	0.481
T=2000	0.814	0.786	0.732	0.698
H = 10				
T=500	0.356	0.363	0.342	0.311
T=1000	0.518	0.489	0.473	0.444
T=2000	0.750	0.741	0.685	0.667

Notes: For a given value of the quadruplet (α, H, T, M) the Table displays the empirical power of the Granger-causality test in extreme integrated variance, with α the confidence level, T the sample size (in days), M the number of intraday returns used to compute the realized measure of integrated variance, and H the maximum lag-order for the causality test. Under the alternative hypothesis, we allow for causality in both the IV and the jump processes. The nominal significance level η is set to 5%. The rejection frequencies are computed over 1000 simulations.

Table 9: Empirical power of the causality test in extreme variance for the RK measure

$\alpha = 90\%$				
	$M = 390$	$M = 78$	$M = 26$	$M = 13$
H = 3				
T=500	0.602	0.555	0.473	0.416
T=1000	0.921	0.874	0.803	0.708
T=2000	1.000	0.991	0.971	0.944
H = 5				
T=500	0.554	0.490	0.417	0.362
T=1000	0.877	0.839	0.747	0.643
T=2000	1.000	0.988	0.957	0.918
H = 10				
T=500	0.438	0.368	0.335	0.273
T=1000	0.804	0.737	0.624	0.528
T=2000	0.991	0.971	0.928	0.866
$\alpha = 95\%$				
	$M = 390$	$M = 78$	$M = 26$	$M = 13$
H = 3				
T=500	0.391	0.345	0.305	0.284
T=1000	0.638	0.591	0.526	0.450
T=2000	0.904	0.852	0.789	0.709
H = 5				
T=500	0.308	0.284	0.249	0.214
T=1000	0.585	0.530	0.470	0.405
T=2000	0.875	0.823	0.746	0.643
H = 10				
T=500	0.284	0.274	0.216	0.196
T=1000	0.491	0.438	0.377	0.307
T=2000	0.779	0.739	0.636	0.532

Notes: For a given value of the quadruplet (α, H, T, M) the Table displays the empirical power of the Granger-causality test in extreme quadratic variation, with α the confidence level, T the sample size (in days), M the number of intraday returns used to compute the realized measure of quadratic variation, and H the maximum lag-order for the causality test. Under the alternative hypothesis, there is no causality in the IV but we allow for spillovers in the jumps process. The nominal significance level η is set to 5%. The rejection frequencies are computed over 1000 simulations.

Table 10: Empirical size of the causality test in extreme variance for the BV measure

$\alpha = 90\%$				
	$M = 390$	$M = 78$	$M = 26$	$M = 13$
H = 3				
T=500	0.040	0.044	0.056	0.069
T=1000	0.045	0.046	0.073	0.095
T=2000	0.042	0.060	0.114	0.153
H = 5				
T=500	0.047	0.046	0.055	0.067
T=1000	0.053	0.047	0.065	0.086
T=2000	0.048	0.058	0.107	0.141
H = 10				
T=500	0.047	0.040	0.052	0.057
T=1000	0.055	0.049	0.053	0.074
T=2000	0.048	0.052	0.093	0.106
$\alpha = 95\%$				
	$M = 390$	$M = 78$	$M = 26$	$M = 13$
H = 3				
T=500	0.057	0.076	0.098	0.100
T=1000	0.053	0.065	0.078	0.099
T=2000	0.051	0.066	0.09	0.106
H = 5				
T=500	0.060	0.070	0.077	0.080
T=1000	0.062	0.069	0.082	0.096
T=2000	0.055	0.069	0.079	0.099
H = 10				
T=500	0.069	0.065	0.094	0.087
T=1000	0.054	0.060	0.074	0.076
T=2000	0.054	0.062	0.086	0.080

Notes: For a given value of the quadruplet (α, H, T, M) the Table displays the empirical size of the Granger-causality test in extreme integrated variance, with α the confidence level, T the sample size (in days), M the number of intraday returns used to compute the realized measure of integrated variance, and H the maximum lag-order for the causality test. Under the alternative hypothesis, there is no causality in the IV but we allow for spillovers in the jumps process. The nominal significance level η is set to 5%. The rejection frequencies are computed over 1000 simulations.

Table 11: Regression results

	β_0	β_1	β_2	δ_1
FTSE	2.488 (19.94)	0.181 (10.81)	-0.033 (-0.858)	0.019 (1.107)
DAX	2.516 (14.14)	0.197 (8.331)	-0.051 (-1.340)	0.047 (3.338)
CAC	2.809 (10.70)	0.179 (8.064)	-0.093 (-1.368)	0.035 (1.079)
AEX	2.661 (16.58)	0.193 (6.818)	-0.072 (-1.606)	0.031 (1.174)
IBEX	2.392 (22.33)	0.175 (9.275)	-0.004 (-0.132)	-0.002 (-0.098)
MIB	2.858 (20.33)	0.226 (12.16)	-0.107 (-2.738)	-0.053 (-1.338)

Notes: The estimated regression is $\log \widehat{Q}(H) = \beta_0 + \beta_1 SR \mathbb{I}_{\widehat{Q}(H) > \chi_{95\%}^2(H)} + \beta_2 SR + \delta_1 TEDS + \varepsilon$, with SR representing the range of the US shadow rate and $TEDS$ a control variable. The test statistic $\widehat{Q}(H)_t$ is obtained by setting α to 95% and $H = 10$ lags in a rolling windows setup with $T = 500$ on 5-minutes bi-power variation. HAC t-statistics are computed by following Sun (2004) with a bandwidth of 0.1 and displayed between parentheses.